

Stochastic approximation of high-molecular by bi-molecular reactions

Tomislav Plesa*

Abstract: Biochemical networks, under mass-action kinetics, containing reactions with three or more reactants (called high-molecular reactions) are investigated. An algorithm for stochastically approximating the high-molecular reactions with a set of bi-molecular ones, involving at most two reactants, is presented. Properties of the algorithm and convergence are established by applying singular perturbation theory on the underlying chemical master equation. The algorithm is applied to a variety of examples from both systems and synthetic biology, demonstrating that biochemically plausible bi-molecular reaction networks may display a variety of noise-induced phenomena, and may be designed in a systematic manner.

1 Introduction

Reaction networks [1, 2] are a central mathematical framework utilized for analyzing biochemical circuits from systems biology [3, 4, 5], and are a powerful programming language for designing synthetic molecular systems [6, 7, 8, 9, 10]. Molecular networks in the context of classical biochemistry typically do not include reactions of order three or higher (referred to in this paper as higher-order, or high-molecular, reactions), since reactive collisions between three or more molecules are unlikely to take place [2, 11]. However, let us note that the higher-order reactions are in principle realizable in the context of nucleic-acid-based synthetic biology [12]. Despite the overall experimental implausibility of such reactions, they appear in both theoretical systems and synthetic biology. For example, third-order (tri-molecular) reactions appear in the Schlögl system [13], where they allow for bistationarity (coexistence of two stable equilibria), in the Brusselator [14] and Schnakenberg systems [15], which display oscillations (existence of a stable limit cycle), as well as in two-species networks displaying bicyclicity (coexistence of two stable limit cycles) [16], and a variety of bifurcation structures, such as homoclinic and saddle-node on invariant circle (SNIC) bifurcations [8, 17]. Aside from well-mixed settings, third-order reactions also play a role in pattern formation [18], and, more broadly, are a subject of research within reaction-diffusion modeling in systems biology [19]. On the other hand, in synthetic biology, higher-order reactions appear e.g. in the so-called noise-control algorithm, put forward in [9], where such reactions allow for a precise state-dependent control of the biochemical stochastic dynamics. In order to experimentally realize the higher-order reactions in synthetic biology, they should, in general, first be mapped to suitable second-order (bi-molecular) reactions [6]. In the context of systems biology, such a mapping allows for a biochemical interpretation of higher-order reactions. Thus, it is of both practical and theoretical interest to develop a suitable order-reduction algorithm, mapping high-molecular into bi-molecular networks.

An algorithm for approximating higher-order reaction networks by second-order ones at the *deterministic level* (i.e. at the level of reaction-rate equations) has been used for decades, e.g. see [20, 21, 22, 23]. The algorithm has been rigorously justified in the deterministic setting in [24, Section 3] for general third- and fourth-order reactions using perturbation theory. Its performance depends upon an asymptotic parameter, appearing as a rate coefficient of some of the underlying

* Department of Bioengineering, Imperial College London, Exhibition Road, London, SW7 2AZ, UK; e-mail: tplesa@ic.ac.uk

chemical reactions. Another, more elaborate, order-reduction procedure has been presented in [25, 26]. While the latter procedure does not depend on an asymptotic parameter, it depends on the precise initial conditions of some of the underlying species, which, from the perspective of synthetic biology, may pose significant challenges [27, 28]. Less attention has been paid to the validity of such approximations at the *stochastic level* (i.e. at the level of the chemical master equation (CME) [29]): it has been formally shown in [30] that the specific third-order reaction, given by $3s \rightarrow 2s$, may be stochastically approximated by a second-order network using the algorithm from [24], and this has also been qualitatively described in [11]. However, the questions of whether the formal deterministic results from [24] extend into the stochastic setting, and whether dynamics of the approximating second-order networks converge in a suitable limit to the dynamics of the original higher-order network, remain unanswered. In particular, validity of perturbation results at the deterministic level does not generally guarantee validity at the stochastic level [31, 32, 33].

In this paper, we apply singular perturbation theory involving the CME, known in the context of chemical reaction networks as stochastic quasi-stationary approximations (QSAs) [34, 35], in order to show that networks of arbitrarily high-order may be approximated by second-order ones at the stochastic level using the algorithm from [24]. The paper is organized as follows. In Section 2, we start by showing that any third-order reaction, involving identical reactants, may be approximated stochastically by a family of second-order networks, stated as Lemma 2.1. In Section 2.3, we apply Lemma 2.1 on the Schlögl system [13], given as the third-order test network (23), which displays both deterministic and stochastic bistabilities for the chosen rate coefficients. We demonstrate that an approximating second-order network displays the same stationary probability mass function (PMF) and switching pattern between the two PMF maxima as the original third-order network in an asymptotic limit (see also Figures 1 and 2). In Section 3, we show that reaction networks of arbitrarily high order may be stochastically approximated by a family of second-order networks, by generalizing Lemma 2.1 to Theorem 3.1, and establish a weak-convergence result in Theorem 3.2 for a particular sub-family of the approximating second-order networks. We also present two extended examples in Sections 3.1 and 3.2, involving applications of Theorem 3.1 to the test networks (44) and (48), respectively, which display purely stochastic phenomena, and demonstrate validity of Theorem 3.1 (see also Figure 3). The notation used in the paper is introduced as needed, and is summarized in Appendix A. Proofs of Theorems 3.1 and 3.2 can be found in Appendices B and C, respectively.

2 Special case: Third-order homoreactions

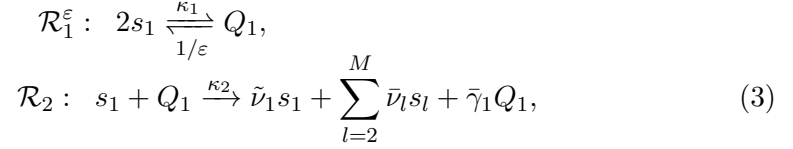
Let us start our analysis by considering an arbitrary third-order (tri-molecular) *homoreaction*, i.e. a reaction involving three reactant molecules of *the same species*, under mass-action kinetics, which is given by



where $\{s_l\}_{l=1}^N$ are the interacting biochemical species, $\{\bar{\nu}_l\}_{l=1}^N \in \mathbb{Z}_{\geq}$ the stoichiometric coefficients, and $k \in \mathbb{R}_{>}$ is a dimensionless rate coefficient, where \mathbb{Z}_{\geq} , and $\mathbb{R}_{>}$, denote the set of non-negative integers, and positive real numbers, respectively (see also Appendix A). Let us also consider the second-order (bi-molecular) network, under mass-action kinetics, given by

$$\mathcal{R}_{\varepsilon} = \mathcal{R}_1^{\varepsilon} \cup \mathcal{R}_2, \quad (2)$$

with the sub-networks



where Q_1 is an auxiliary species, $\tilde{\nu}_1, \bar{\gamma}_1 \in \mathbb{Z}_{\geq}$, and $\kappa_1, \kappa_2, \varepsilon \in \mathbb{R}_{>}$ are positive dimensionless parameters. Here, for convenience, we denote two irreversible reactions $(\nu \rightarrow \bar{\nu}) \in \mathcal{R}$, called the forward reaction, and $(\bar{\nu} \rightarrow \nu) \in \mathcal{R}$, called the backward reaction, jointly as the single reversible reaction $(\nu \rightleftharpoons \bar{\nu}) \in \mathcal{R}$. We say that network (2)–(3) is of second-order, because its highest-order reaction is of second-order (see also Appendix A). For mathematical convenience, we also define the fast sub-network



In what follows, we assume ε is a small parameter, $0 < \varepsilon \ll 1$, and that the rate coefficients of the forward reaction from $\mathcal{R}_1^\varepsilon$ and reaction \mathcal{R}_2 are much smaller than the rate coefficient of the backward reaction from $\mathcal{R}_1^\varepsilon$ for sufficiently small ε , i.e. $\kappa_1, \kappa_2 \ll 1/\varepsilon$ as $\varepsilon \rightarrow 0$. We now proceed to use perturbation theory to formally show that, under appropriate conditions, stochastic dynamics of the third-order input network (1) and the second-order output network (2)–(3) are approximately the same in a weak sense. To this end, let us first introduce the chemical master equation (CME) [36, 37, 38] of the output network (see also Appendix A).

The chemical master equation. Let $\mathbf{x} = (x_1, x_2, \dots, x_N) \in \mathbb{Z}_{\geq}^N$ be the vector of copy-numbers of the species s_1, s_2, \dots, s_N , and $y_1 \in \mathbb{Z}_{\geq}$ the copy-number of the auxiliary species Q_1 , appearing in the network (2)–(3). The forward operator of the fast sub-network $\mathcal{R}_0^\varepsilon$ is given by $\mathcal{L}_0 = 1/\varepsilon(E_{x_1}^{-2}E_{y_1}^{+1} - 1)y_1$, where $E_x^{-\Delta x}$ is a step-operator such that $E_x^{-\Delta x}p(x, t) = p(x - \Delta x, t)$ (see also Appendix A). The fast process has a linear conservation law: $x_1 + 2y_1 = \bar{x}_1$, where \bar{x}_1 is a time-independent constant for the process induced by \mathcal{L}_0 . Let us introduce a new vector $\bar{\mathbf{x}} = (\bar{x}_1, x_2, \dots, x_N) \in \mathbb{Z}_{\geq}^N$, with the first coordinate given by

$$\bar{x}_1 = x_1 + 2y_1. \quad (5)$$

Under the coordinate transformation (5), the fast sub-network (4) simplifies to the network $Q_1 \rightarrow \emptyset$, with the forward operator $\mathcal{L}_0 = 1/\varepsilon(E_{y_1}^{+1} - 1)y_1$

The CME, governing the time-evolution of the probability mass function (PMF) underlying the network (2)–(3), on the slow time-scale $\tau = \mathcal{O}(1)$, defined by $t = \tau/\varepsilon$ (the time is rescaled in order to capture nontrivial dynamics, as explained in what follows), and expressed in terms of the new coordinates $\bar{\mathbf{x}}$, reads

$$\frac{\partial}{\partial \tau} p_\varepsilon(\bar{\mathbf{x}}, y_1, \tau) = \left(\frac{1}{\varepsilon^2} \mathcal{L}_0 + \frac{1}{\varepsilon} \mathcal{L}_1 \right) p_\varepsilon(\bar{\mathbf{x}}, y_1, \tau). \quad (6)$$

Here, operators \mathcal{L}_0 , and \mathcal{L}_1 , are induced by the fast sub-network \mathcal{R}_0^1 , and the remaining (slow) sub-network $\mathcal{R}_\varepsilon \setminus \mathcal{R}_0^\varepsilon$, respectively, and given by

$$\begin{aligned} \mathcal{L}_0 &= (E_{y_1}^{+1} - 1) y_1, \\ \mathcal{L}_1 &= (E_{y_1}^{-1} - 1) \alpha_1(\bar{x}_1, y_1) + \left(E_{\bar{\mathbf{x}}}^{-\Delta \bar{\mathbf{x}}} E_{y_1}^{-\Delta y_1} - 1 \right) y_1 \alpha_2(\bar{x}_1, y_1). \end{aligned} \quad (7)$$

Functions $\alpha_1(\bar{x}_1, y_1)$, and $y_1\alpha_2(\bar{x}_1, y_1)$, are the propensity functions of the reactions from $\mathcal{R}_\varepsilon \setminus \mathcal{R}_0^\varepsilon$, expressed in terms of (5), with

$$\begin{aligned}\alpha_1(\bar{x}_1, y_1) &= \kappa_1 x_1 (x_1 - 1) = \kappa_1 (\bar{x}_1 - 2y_1)(\bar{x}_1 - 2y_1 - 1), \\ \alpha_2(\bar{x}_1, y_1) &= \kappa_2 x_1 = \kappa_2 (\bar{x}_1 - 2y_1).\end{aligned}\tag{8}$$

The jump vector $\Delta\bar{\mathbf{x}}$ is given by $\Delta\bar{\mathbf{x}} = (\Delta\bar{x}_1, \bar{\nu}_2, \dots, \bar{\nu}_N)$, where $\Delta\bar{x}_1$ may be formally obtained by applying the difference operator Δ on (5), and reads

$$\Delta\bar{x}_1 = \Delta x_1 + 2\Delta y_1 = (\bar{\nu}_1 - 1) + 2(\bar{\gamma}_1 - 1).\tag{9}$$

2.1 Perturbation analysis

Let us write the solution of (6) as the perturbation series

$$p_\varepsilon(\bar{\mathbf{x}}, y_1, \tau) = p_0(\bar{\mathbf{x}}, y_1, \tau) + \varepsilon p_1(\bar{\mathbf{x}}, y_1, \tau) + \varepsilon^2 p_2(\bar{\mathbf{x}}, y_1, \tau) + \dots\tag{10}$$

We require the *zero-order approximation* $p_0(\bar{\mathbf{x}}, y_1, \tau)$ from (10) to be a PMF (i.e. it must be nonnegative and normalized). Substituting (10) into (6), and equating terms of equal powers in ε , the following system of three equations is obtained:

$$\begin{aligned}\mathcal{O}(1/\varepsilon^2) : \mathcal{L}_0 p_0(\bar{\mathbf{x}}, y_1, \tau) &= 0, \\ \mathcal{O}(1/\varepsilon) : \mathcal{L}_0 p_1(\bar{\mathbf{x}}, y_1, \tau) &= -\mathcal{L}_1 p_0(\bar{\mathbf{x}}, y_1, \tau), \\ \mathcal{O}(1) : \mathcal{L}_0 p_2(\bar{\mathbf{x}}, y_1, \tau) &= \frac{\partial}{\partial \tau} p_0(\bar{\mathbf{x}}, y_1, \tau) - \mathcal{L}_1 p_1(\bar{\mathbf{x}}, y_1, \tau).\end{aligned}\tag{11}$$

The first equation in (11) is homogeneous, and forms a zero-eigenvalue problem, while the remaining two are inhomogeneous.

Order $1/\varepsilon^2$ equation. It follows from the structure of \mathcal{L}_0 that we may write $p_0(\bar{\mathbf{x}}, y_1, \tau) = p_0(y_1)p_0(\bar{\mathbf{x}}, \tau)$. Assuming $p_0(\bar{\mathbf{x}}, \tau) > 0$ for any $\bar{\mathbf{x}} \in \mathbb{Z}_{\geq}^N$ and any $\tau > 0$, the first equation from (11) reduces to $\mathcal{L}_0 p_0(y_1) = 0$. Operator \mathcal{L}_0 has a one-dimensional null-space, $\mathcal{N}(\mathcal{L}_0) = \{1_{y_1} \delta_{y_1, 0}\}$, where 1_{y_1} denotes functions independent of y_1 , and $\delta_{i,j}$ is the Kronecker-delta function, non-zero only at $i = j$, where it is equal to one. We seek an element of this one-dimensional space which is normalized, resulting in

$$p_0(\bar{\mathbf{x}}, y_1, \tau) = p_0(\bar{\mathbf{x}}, \tau) \delta_{y_1, 0}, \quad \sum_{\bar{\mathbf{x}}} p_0(\bar{\mathbf{x}}, \tau) = 1, \quad \text{for } \tau \geq 0.\tag{12}$$

In other words, under the infinitely fast reaction $Q_1 \rightarrow \emptyset$, the y_1 -marginal PMF is concentrated at zero, making Q_1 a short-lived species.

Order $1/\varepsilon$ equation. Using (7) and (12), the right-hand side (RHS) of the second equation from (11) becomes

$$\mathcal{L}_1 p_0(\bar{\mathbf{x}}, y_1, \tau) = p_0(\bar{\mathbf{x}}, \tau) (E_{y_1}^{-1} - 1) \alpha_1(\bar{x}_1, y_1) \delta_{y_1, 0}.\tag{13}$$

Let us denote the l^2 -adjoint operator of \mathcal{L}_0 by \mathcal{L}_0^* , called the backward operator, which is given by $\mathcal{L}_0^* = y_1 (E_{y_1}^{-1} - 1)$ (see Appendix A). The second equation from (11) has either no solutions or infinitely many solutions, since the backward operator \mathcal{L}_0^* has a non-trivial null-space, given by $\mathcal{N}(\mathcal{L}_0^*) = \{1_{y_1}\}$. In order to achieve the latter, the Fredholm alternative theorem [39] implies

that the RHS of the equation has to be orthogonal to the null-space of the backward operator \mathcal{L}_0^* . Using (13), the solvability condition becomes

$$0 = \langle 1_{y_1}, \mathcal{L}_1 p_0(\bar{\mathbf{x}}, y_1, \tau) \rangle = \langle (E_{y_1}^{+1} - 1)1_{y_1}, \alpha_1(\bar{x}_1, y_1)p_0(\bar{\mathbf{x}}, y_1, \tau) \rangle \quad (14)$$

where $\langle f, g \rangle = \sum_{y_1=0}^{\infty} f(y_1)g(y_1)$ denotes an l^2 inner-product. Constraint (14) is unconditionally satisfied, since $(E_{y_1}^{+1} - 1)1_{y_1} = 0$. Note that if the time had not been rescaled according to $t = \tau/\varepsilon$ in (6), the second equation from (11) would read $\mathcal{L}_0 p_1(\bar{\mathbf{x}}, y_1, t) = (\frac{\partial}{\partial t} - \mathcal{L}_1)p_0(\bar{\mathbf{x}}, y_1, t)$, and the solvability condition would give a trivial effective CME, $\frac{\partial}{\partial t}p_0(\bar{\mathbf{x}}, t) = 0$. For this reason, we have rescaled the time to a longer scale.

Since the operator \mathcal{L}_0 acts only on y_1 variable, and because of equality (13), the solution of the second equation in (11) may be written in the separable form

$$p_1(\bar{\mathbf{x}}, y_1, \tau) = p_0(\bar{\mathbf{x}}, \tau)p_1(y_1; \bar{\mathbf{x}}). \quad (15)$$

Note that the factor $p_1(y_1; \bar{\mathbf{x}})$ generally cannot be interpreted as a (conditional) PMF (e.g. it may be negative), and hence we write $p_1 = p_1(y_1; \bar{\mathbf{x}})$ instead of $p_1 = p_1(y_1|\bar{\mathbf{x}})$. Substituting (15) into the second equation in (11), using (13) and the operator equality $(E_{y_1}^{-1} - 1) = -(E_{y_1}^{+1} - 1)E_{y_1}^{-1}$, and assuming positivity of $p_0(\bar{\mathbf{x}}, \tau)$, one obtains

$$(E_{y_1}^{+1} - 1)(y_1 p_1(y_1; \bar{\mathbf{x}}) - E_{y_1}^{-1} \alpha_1(\bar{x}_1, y_1) \delta_{y_1,0}) = 0,$$

implying that the solutions $p_1(y_1; \bar{\mathbf{x}})$ satisfy

$$y_1 p_1(y_1; \bar{\mathbf{x}}) = E_{y_1}^{-1} \alpha_1(\bar{x}_1, y_1) \delta_{y_1,0}. \quad (16)$$

Order 1 equation. The solvability condition for the third equation from (11) is given by

$$0 = \left\langle 1, \frac{\partial}{\partial \tau} p_0(\bar{\mathbf{x}}, y_1, \tau) \right\rangle - \langle 1, \mathcal{L}_1 p_1(\bar{\mathbf{x}}, y_1, \tau) \rangle. \quad (17)$$

Equation (12) implies that the first term from (17) reads $\langle 1, \partial/\partial \tau p_0(\bar{\mathbf{x}}, y_1, \tau) \rangle = \partial/\partial \tau p_0(\bar{\mathbf{x}}, \tau)$. Using equations (7) and (15), the second term from (17) reads

$$\langle 1, \mathcal{L}_1 p_1(\bar{\mathbf{x}}, y_1, \tau) \rangle = (E_{\bar{\mathbf{x}}}^{-\Delta \bar{\mathbf{x}}} - 1) p_0(\bar{\mathbf{x}}, \tau) \langle 1, \alpha_2(\bar{x}_1, y_1) (y_1 p_1(y_1; \bar{\mathbf{x}})) \rangle,$$

which, upon substituting (16), becomes

$$\langle 1, \mathcal{L}_1 p_1(\bar{\mathbf{x}}, y_1, \tau) \rangle = (E_{\bar{\mathbf{x}}}^{-\Delta \bar{\mathbf{x}}} - 1) \alpha_1(\bar{x}_1, 0) \alpha_2(\bar{x}_1, 1) p_0(\bar{\mathbf{x}}, \tau). \quad (18)$$

Substituting (18) into (17), using (8), and changing the time back to the original scale, $\tau = \varepsilon t$, one obtains the *effective* CME

$$\frac{\partial}{\partial t} p_0(\bar{\mathbf{x}}, t) = \left(E_{\bar{\mathbf{x}}}^{-\Delta \bar{\mathbf{x}}} - 1 \right) \varepsilon \kappa_1 \kappa_2 \bar{x}_1 (\bar{x}_1 - 1) (\bar{x}_1 - 2) p_0(\bar{\mathbf{x}}, t). \quad (19)$$

The presence of the factor ε on the RHS of the effective CME (19) stems from the fact that non-trivial dynamics (i.e. an effective CME with a non-zero RHS) occur at $t = \mathcal{O}(1/\varepsilon)$. Put it another way, the most common firing pattern of the network \mathcal{R}_ε , given by (2)–(3), consists of a firing of the reaction $2s_1 \rightarrow Q_1$, which produces the short-lived species Q_1 , followed by the fast reaction $Q_1 \rightarrow 2s_1$, which quickly converts Q_1 back to $2s_1$, which leads to a trivial dynamics of s_1 . However, after long enough time, another firing pattern is also occasionally observed: after Q_1 is produced from $2s_1$, instead of being quickly converted back to $2s_1$, it participates in the target slow reaction $s_1 + Q_1 \rightarrow \tilde{\nu}_1 s_1 + \sum_{l=2}^M \bar{\nu}_l s_l + \bar{\gamma}_1 Q_1$, which gives rise to non-trivial dynamics of s_1 .

2.2 Validity of the effective CME

Let us now compare the CME of the input network (1) with the effective CME of the output network (2)–(3), given by (19). Before doing so, note that (19) is expressed in terms of the variable \bar{x}_1 , defined in (5), and not the original copy-number x_1 . Denoting by $Y_1(t)$ the time-dependent copy-number of Q_1 , and assuming convergence of the perturbation series (10) (see also Theorem 3.2 in Section 3), it follows from (12) that $Y_1(t)$ converges to zero. As a consequence, equation (5) implies that $\bar{X}_1(t)$ converges to $X_1(t)$ as $\varepsilon \rightarrow 0$, so that we may replace \bar{x}_1 by x_1 in (19), ensuring that the effective CME describes copy-number of the species s_1 .

Stoichiometric and kinetic conditions. The effective propensity function appearing in (19) is given by $\alpha_{\text{eff}}(x) \equiv \varepsilon\kappa_1\kappa_2x_1(x_1 - 1)(x_1 - 2)$. It has the same form as the the propensity function of the input network (1), given by $\alpha(x) \equiv kx_1(x_1 - 1)(x_1 - 2)$. However, the input reaction and the effective output reaction generally have different reaction vectors and rate coefficients. In order for the effective CME (19) of the network (2)–(3) to match the CME of network (1), we must hence require two conditions. Firstly, we require that the effective reaction vector element $\Delta\bar{x}_1$, given by (9), is equal to the original one, $\Delta x_1 = \bar{\nu}_1 - 3$. This imposes the *stoichiometric condition* on $\tilde{\nu}_1$ and $\tilde{\gamma}_1$:

$$\tilde{\nu}_1 = \bar{\nu}_1 - 2\tilde{\gamma}_1. \quad (20)$$

Secondly, we require that the effective propensity function is equal to the original one. This imposes the *kinetic condition*:

$$\varepsilon\kappa_1\kappa_2 = k, \quad \text{with } \varepsilon\kappa_1, \varepsilon\kappa_2 \ll 1, \quad \text{for } 0 < \varepsilon \ll 1. \quad (21)$$

Let us now summarize the established results.

Lemma 2.1. *Consider the third-order input network \mathcal{R}_0 , given by (1), and the second-order output network \mathcal{R}_ε , given by (2)–(3). The \mathbf{x} -marginal zero-order PMF of the output network \mathcal{R}_ε , with $0 < \varepsilon \ll 1$, from the perturbation series (10), satisfies the effective CME (19). Furthermore, assume the stoichiometric and kinetic conditions (20) and (21) are satisfied, respectively. Then, the effective CME (19) of the output network \mathcal{R}_ε is identical to the CME of the input network \mathcal{R}_0 .*

Convergence. Lemma 2.1 provides conditions under which the effective CME of the output network matches the CME of the input network. This has been obtained by means of formal asymptotics, under the assumption that the rate coefficients $\kappa_1, \kappa_2 \ll 1/\varepsilon$, with $0 < \varepsilon \ll 1$. In order to establish convergence of the perturbation series (10) as $\varepsilon \rightarrow 0$, one may choose the coefficients κ_1 and κ_2 according to (21), expand the PMF of the output network into an appropriate perturbation series, and then study a convergence. For example, by choosing $\kappa_1 = \tilde{\kappa}_1\varepsilon^{-1/2}$ and $\kappa_2 = \tilde{\kappa}_2\varepsilon^{-1/2}$, with $\tilde{\kappa}_1\tilde{\kappa}_2 = k$, one obtains

$$\|p_\varepsilon(\mathbf{x}, y_1, t) - p_0(\mathbf{x}, y_1, t)\|_1 = \mathcal{O}(\varepsilon^{\frac{1}{2}}), \quad \text{as } \varepsilon \rightarrow 0, \quad (22)$$

for any finite-time interval, where $\|\cdot\|_1$ denotes the l^1 -norm over the bounded state-spaces of \mathbf{x} and \mathbf{y} , which we prove in a more general setting in Section 3 (in particular, see Theorem 3.2 with $n = 3$). Different scalings of κ_1 and κ_2 generally lead to different orders of convergence. For example, one can readily show that choosing $\kappa_1 = \mathcal{O}(\varepsilon^{-1/3})$ and $\kappa_2 = \mathcal{O}(\varepsilon^{-2/3})$ leads to a slower convergence: $\|p_\varepsilon(\mathbf{x}, y_1, t) - p_0(\mathbf{x}, y_1, t)\|_1 = \mathcal{O}(\varepsilon^{\frac{1}{3}})$, for sufficiently small ε . In general, the convergence is limited by the slowest reaction in the output network (3).

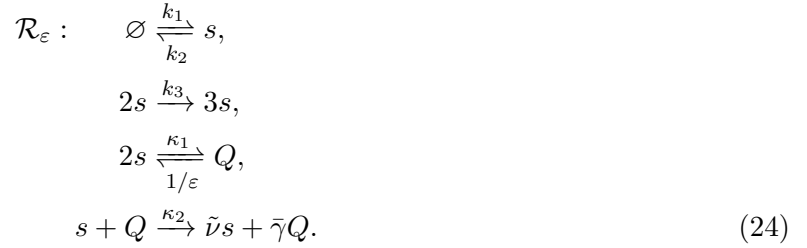
Assuming convergence, Lemma 2.1 implies that the statistics of the common species from the input and output networks are close for each fixed *finite-time* interval, when $0 < \varepsilon \ll 1$. In the next section, we numerically investigate how well the *long-time* statistics of the input and output networks match for a particular test model.

2.3 Example: The Schlögl system

Let us consider the one-species third-order input reaction network, known as the Schlögl system [13], given by



For particular choices of the rate coefficients, system (23) is deterministically bistationary (displays two coexisting stable equilibria), and stochastically bimodal (the underlying PMF displays two maxima) [13, 17], and, in what follows, we consider such a choice of the dimensionless rate coefficients: $(k_1, k_2, k_3, k_4) = (1125, 37.5, 0.36, 10^{-3})$. Let us approximate the input network (23) with a second-order output network by applying Lemma 2.1 on the third-order reaction $3s \rightarrow 2s$, leading to the output network



Using the notation from (3), $\mathcal{R}_1^\varepsilon : 2s \rightleftharpoons Q$, and $\mathcal{R}_2 : s + Q \rightarrow \tilde{\nu}s + \bar{\gamma}Q$. Let us impose the stoichiometric and kinetic conditions on the network (24), as specified in Lemma 2.1. In particular, the stoichiometric condition, given by (20), implies $\tilde{\nu} = (2 - 2\bar{\gamma})$, and there are two options: (i) taking $\bar{\gamma} = 0$ implies $\tilde{\nu} = 2$, (ii) taking $\bar{\gamma} = 1$ implies $\tilde{\nu} = 0$, while increasing $\bar{\gamma}$ further leads to $\tilde{\nu} < 0$, which is chemically unfeasible. On the other hand, the kinetic condition, given by (21), implies $\varepsilon\kappa_1\kappa_2 = k_4$. In what follows, we consider (24) with $(\tilde{\nu}, \bar{\gamma}) = (0, 1)$, and $\kappa_1 = \kappa_2 = \varepsilon^{-1/2}\sqrt{k_4}$, and we denote copy-numbers of the species s and Q by x and y , respectively.

Stationary PMF. Let us compare the stationary PMFs of the input network (23), denoted by $p_0 = p_0(x)$, with the x -marginal stationary PMF of the output network (24), denoted by $p_{\varepsilon,x} = p_{\varepsilon,x}(x)$, which capture the long-time behavior of the systems, and are thus of practical importance. In Figure 1(a), we display the stationary PMF $p_{\varepsilon,x}(x)$ for various values of the asymptotic parameter ε . In particular, we show the input (target) PMF $p_0(x)$ as the black curve, while the output PMF $p_{\varepsilon,x}(x)$ for $\varepsilon = 10^{-3}$ and $\varepsilon = 10^{-6}$ as the dashed purple curve and the blue histogram, respectively. When $\varepsilon = 10^{-3}$, the output PMF is bimodal, but the PMF is inaccurately distributed. Such a mismatch arises from the fact that the asymptotic parameter is not sufficiently small: $1/\varepsilon$ should be larger than the largest rate coefficient appearing in the input network (23) (which is $k_3 = \mathcal{O}(10^3)$). On the other hand, when $\varepsilon = 10^{-6}$, i.e. when $1/\varepsilon$ is three orders of magnitude higher than k_3 , the matching between the input and output networks is excellent. In Figure 1(b), we show the y -marginal PMF for the output network when $\varepsilon = 10^{-6}$, and one can notice that it is concentrated around $y = 0$. In Figures 1(c)–(d), we show representative sample paths corresponding to the histograms from (a)–(b), respectively, where one can notice a stochastic switching phenomenon for the species s .

To gain more quantitative information, let us measure the distance (error) between the input

and output PMFs as a function of the asymptotic parameter ε by using the l^1 -norm:

$$\|p_{\varepsilon,x} - p_0\|_1 = \sum_x |p_{\varepsilon,x}(x) - p_0(x)|. \quad (25)$$

In Figure 2(a), we display a log-log plot of $\|p_{\varepsilon,x} - p_0\|_1$, as a function of the asymptotic parameter ε , as the black dots interpolated with the black lines, which was obtained by numerically solving the underlying stationary CMEs. We also show as the dashed blue line a log-log plot of the reference curve $\|p_{\varepsilon,x} - p_0\|_1 = \sqrt{\varepsilon}$. One can notice an excellent match in the slopes of the two curves, in accordance with equation (22). In Figure 2(b), we plot the stationary y -marginal PMF evaluated at zero, $p_{\varepsilon,y}(0)$, which converges to 1 as $\varepsilon \rightarrow 0$, in agreement with (12) and (22).

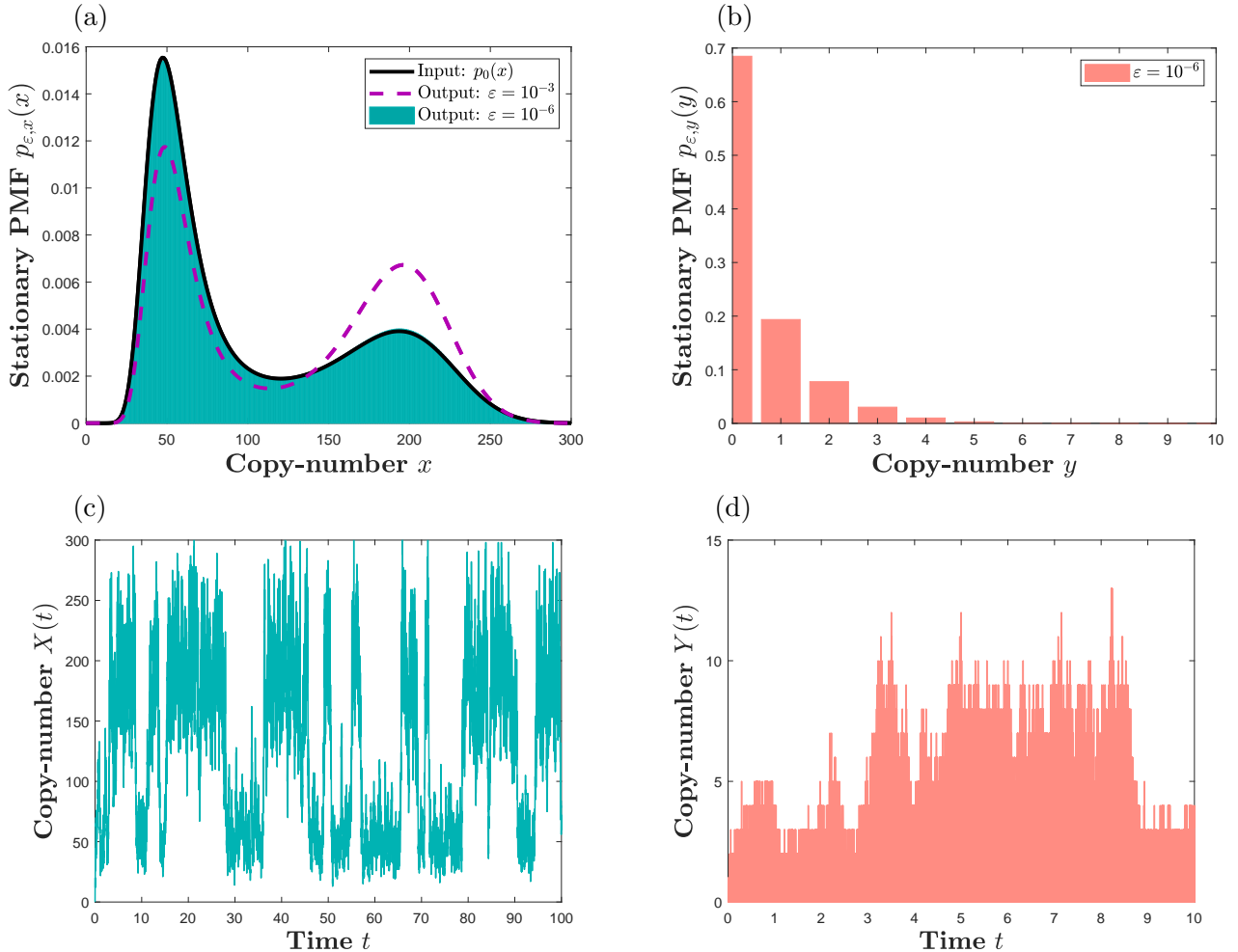


Figure 1: Panel (a) displays the stationary PMF of the input network (23) as the black curve, and the x -marginal PMF for the output network (24) for different values of the asymptotic parameter ε . Panel (c) shows a representative sample path corresponding to the blue histogram from (a), which displays bistability and stochastic switching. Panels (b), and (d), display the y -marginal PMF for (24), which is concentrated near $y = 0$, and an underlying representative sample path, respectively. The parameters are fixed to: $(k_1, k_2, k_3, k_4) = (1125, 37.5, 0.36, 10^{-3})$, $(\tilde{\nu}, \bar{\gamma}) = (0, 1)$, and $\kappa_1 = \kappa_2 = \varepsilon^{-1/2} \sqrt{k_4}$.

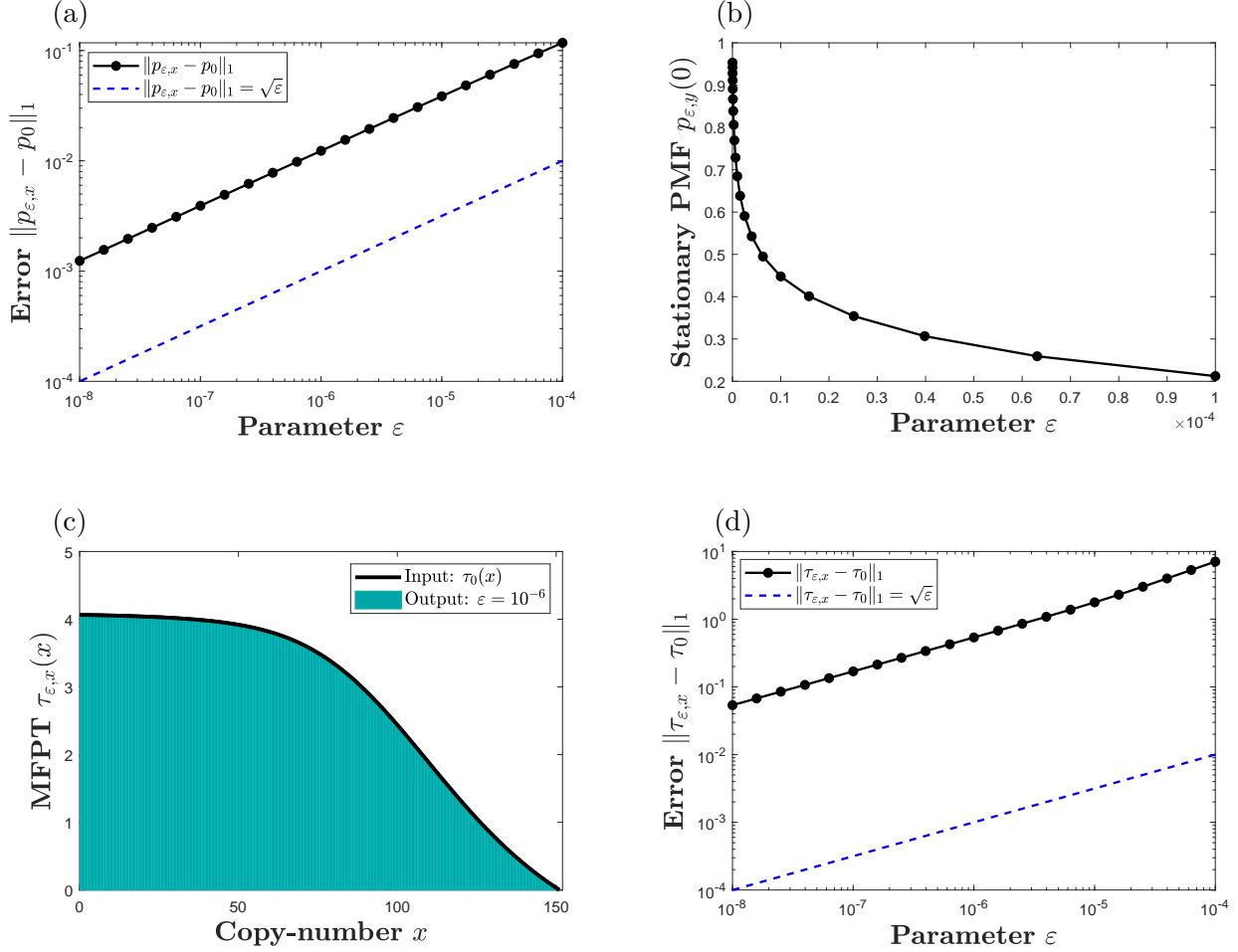


Figure 2: Panel (a) displays as the black dots, interpolated with the black lines, a log-log plot of the l^1 -distance between the PMFs of the input and output networks, given by (23) and (24), respectively, given as equation (25), as a function of the asymptotic parameter ε . Also shown as the dashed blue line is the reference curve $y = \sqrt{\varepsilon}$. Panel (b) shows the y -marginal PMF of the auxiliary species Q from the output network (24), evaluated at $y = 0$, as a function of ε . Panel (c) shows the MFPT for the input network (23) as the black curve, while for the output network (24) as the blue histogram when $\varepsilon = 10^{-6}$. Similar to panel (a), panel (d) displays a log-log plot of the l^1 -distance between mean first passage times (MFPTs) of the input and output networks, obtained by solving equations (26)–(27), as described in the main text. The parameters are fixed as in Figure 1.

Mean first passage time. PMFs provide the probability that the underlying sample paths are at particular states. For multimodal PMFs, another quantity of practical importance is the mean switching time, i.e. the average time it takes the sample paths, starting near one of the PMF maximum, to reach another PMF maximum for the first time. Such information is not provided in Figure 1, as PMFs do not uniquely capture time-parametrization of the underlying sample paths, i.e. sample paths with different switching times may give rise to identical PMFs.

In order to compare the switching times of the input and output networks (23) and (24), respectively, as a function of the asymptotic parameter ε , let us note that the three deterministic equilibria of the input network (23) are approximately given by $(x_{s,1}^*, x_u^*, x_{s,2}^*) \approx (53, 105, 202)$, where $x_{s,1}$ and $x_{s,2}$ are stable, while x_u is the unstable equilibrium. The mean switching time from the lower to the higher PMF modes may be measured by the average time it takes $X(t)$, starting in a neighborhood of $x_{s,1}^*$, to reach $R \approx (x_u^* + x_{s,2}^*)/2$ for the first time [17]. This can be formulated for the input network (23) as the boundary-value problem (BVP) [38]

$$\begin{aligned} \mathcal{L}^* \tau_0(x) &= -1, & x \in [0, R-1], \\ \tau_0(R) &= 0, \end{aligned} \tag{26}$$

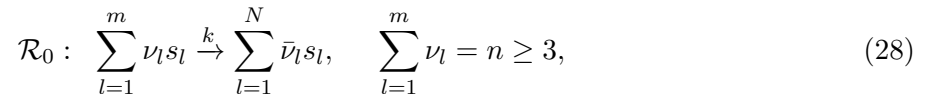
where $\tau_0(x)$ is the mean first passage time (MFPT), given that the initial condition is fixed to x , and \mathcal{L}^* is the backward operator of (23). The second line in (26) is an absorbing boundary condition, expressing the fact that the MFPT, with the starting point $x = R$, is zero. Numerically solving the BVP (26) with $R = 150$ produces the black curve shown in Figure 2(c). Analogous to (26), the BVP for the MFPT of the output network (24), denoted $\tau_\varepsilon(x, y)$, reads:

$$\begin{aligned} \mathcal{L}_\varepsilon^* \tau_\varepsilon(x, y) &= -1, & (x, y) \in [0, R_x - 1] \times [0, R_y], \\ \tau_\varepsilon(R_x, y) &= 0, & y \in [0, R_y], \end{aligned} \tag{27}$$

where $\mathcal{L}_\varepsilon^*$ is the backward operator of (24). We take $R_x = R = 150$, and truncate the y -state-space by taking $R_y = 100$. In what follows, we compare the one-variable quantity $\tau_0(x)$ with the two-variable quantity $\tau_\varepsilon(x, y)$. Since $Y(t)$ spends most of the time at $y = 0$, i.e. since $p_{\varepsilon,y}(y) \approx \delta_{y,0}$ for $0 < \varepsilon \ll 1$, we compare $\tau_0(x)$ with $\tau_{\varepsilon,x}(x) \equiv \tau_\varepsilon(x, 0)$ (i.e. we set the initial condition for y at $y = 0$), and measure the error using the l^1 -norm, $\|\tau_{\varepsilon,x} - \tau_0\|_1$. The error is shown Figure 2(d), and, as predicted by (22), one can notice a $\sqrt{\varepsilon}$ -convergence to zero. In Figure 2(c), we show $\tau_{\varepsilon,x}(x)$ for $\varepsilon = 10^{-6}$ as the blue histogram, which is in an excellent agreement with $\tau_0(x)$ shown in black.

3 General case: n th-order reactions

Let us now consider an arbitrary n th-order reaction, under mass-action kinetics, with m distinct reactants, $\mathcal{R}_0 = \mathcal{R}_0(s_1, s_2, \dots, s_N)$, given by



where we assume the reactant stoichiometric coefficients are positive, $\{\nu_l\}_{l=1}^m \in \mathbb{Z}_{>}$, while the product ones are non-negative, $\{\bar{\nu}_l\}_{l=1}^N \in \mathbb{Z}_{\geq}$, and $N \geq m$. For convenience, it is assumed that the reactant species are ordered according to increasing stoichiometric coefficients, $\nu_l \leq \nu_r$ if $l < r$, for $l, r \in \{1, 2, \dots, m\}$. Let us also consider the second-order reaction network $\mathcal{R}_\varepsilon =$

$\mathcal{R}_\varepsilon(s_1, s_2, \dots, s_N; Q_1, Q_2, \dots, Q_{n-2})$, under mass-action kinetics, given by

$$\mathcal{R}_\varepsilon = \begin{cases} \mathcal{R}_1^\varepsilon(s_1, s_1) \cup \cup_{i=2}^{c_1-2} \mathcal{R}_i^\varepsilon(s_1) \cup \mathcal{R}_{n-1}(s_1), & \text{if } m = 1, \\ \mathcal{R}_1^\varepsilon(s_1, s_2) \cup \cup_{i=2}^{c_1} \mathcal{R}_i^\varepsilon(s_1) \cup \cup_{l=2}^{m-1} \cup_{i=\sum_{j=1}^l c_j-1}^{\sum_{j=1}^l c_j-1} \mathcal{R}_i^\varepsilon(s_l) & \\ \cup \cup_{i=\sum_{j=1}^{m-1} c_j+\delta_{m,2}}^{n-2} \mathcal{R}_i^\varepsilon(s_m) \cup \mathcal{R}_{n-1}(s_m), & \text{if } m \geq 2, \end{cases} \quad (29)$$

with the convention that $\cup_{l=a}^b \mathcal{R}(l) = \emptyset$, if $a < b$, where $\mathcal{R}(l)$ is an arbitrary set indexed by l , and \emptyset is the empty set. The sub-networks from (29) are given by

$$\begin{aligned} \mathcal{R}_1^\varepsilon(s_l, s_r) : \quad & s_l + s_r \xrightleftharpoons[1/\varepsilon]{\kappa_1} Q_1, \\ \mathcal{R}_i^\varepsilon(s_l) : \quad & s_l + Q_{i-1} \xrightleftharpoons[1/\varepsilon]{\kappa_i} Q_i, \quad i \in \{2, 3, \dots, n-2\}, \\ \mathcal{R}_{n-1}(s_r) : \quad & s_r + Q_{n-2} \xrightarrow{\kappa_{n-1}} \sum_{l=1}^m \tilde{\nu}_l s_l + \sum_{l=m+1}^N \bar{\nu}_l s_l + \bar{\gamma}_{n-2} Q_{n-2}, \end{aligned} \quad (30)$$

with $\{\tilde{\nu}_l\}_{l=1}^m, \bar{\gamma}_{n-2} \in \mathbb{Z}_{\geq}$. Network (29)–(30) contains $(n-2)$ auxiliary species $\{Q_i\}_{i=1}^{n-2}$, and consists of $(2n-3)$ reactions: $(n-2)$ first-order faster reactions, and $(n-1)$ second-order slower ones.

In what follows, a generalization of Lemma 2.1 is provided. To this end, we denote the copy-numbers of species s_1, s_2, \dots, s_N by $\mathbf{x} = (x_1, x_2, \dots, x_N) \in \mathbb{Z}_{\geq}^N$, while the copy-numbers of Q_1, Q_2, \dots, Q_{n-2} by $\mathbf{y} = (y_1, y_2, \dots, y_{n-2}) \in \mathbb{Z}_{\geq}^{n-2}$. We consider the perturbation series (64) from Appendix B, where $p_\varepsilon = p_\varepsilon(\mathbf{x}, \mathbf{y}, t)$ is the PMF of the output network (29)–(30), $p_0 = p_0(\mathbf{x}, \mathbf{y}, t)$ its zero-order approximation, while $p_0(\mathbf{x}, t) = \sum_{\mathbf{y}} p_0(\mathbf{x}, \mathbf{y}, t)$ the \mathbf{x} -marginal zero-order PMF.

Theorem 3.1. *Consider the n th-order input network \mathcal{R}_0 , given by (28), and the second-order output network \mathcal{R}_ε , given by (29)–(30). The \mathbf{x} -marginal zero-order PMF of the output network \mathcal{R}_ε , with $0 < \varepsilon \ll 1$, from the perturbation series (64), satisfies the effective CME (83). Furthermore, assume that the parameters $\{\tilde{\nu}_l\}_{l=1}^m$ and $\bar{\gamma}_{n-2}$, from the output network \mathcal{R}_ε , satisfy the stoichiometric conditions*

$$\tilde{\nu}_l = \bar{\nu}_l - (\nu_l - \delta_{l,m})\bar{\gamma}_{n-2}, \quad l \in \{1, 2, \dots, m\}, \quad (31)$$

and that the rate coefficients $\{\kappa_i\}_{i=1}^{n-1}$ satisfy the kinetic condition

$$\varepsilon^{n-2} \prod_{i=1}^{n-1} \kappa_i = k, \quad \varepsilon \kappa_i \ll 1, \quad i \in \{1, 2, \dots, n-1\}, \quad \text{for } 0 < \varepsilon \ll 1. \quad (32)$$

Then, the effective CME of the output network (29)–(30) is identical to the CME of the input network (28).

Proof. See Appendix B. □

Let us also state a convergence result in the case the rate coefficients $\{\kappa_i\}_{i=1}^{n-1}$ are all scaled identically, $\kappa_i = \mathcal{O}(\varepsilon^{-(n-2)/(n-1)})$.

Theorem 3.2. *Consider the output network (29)–(30), satisfying the condition (32), with the following choice of the rate coefficients:*

$$\kappa_i = \tilde{\kappa}_i \varepsilon^{-\left(\frac{n-2}{n-1}\right)}, \quad \prod_{i=1}^{n-1} \tilde{\kappa}_i = k, \quad \tilde{\kappa}_i = \mathcal{O}(1), \quad i \in \{1, 2, \dots, n-1\}. \quad (33)$$

Then, the PMF of the output network converges to its zero-order approximation for any finite-time interval, $p_\varepsilon \rightarrow p_0$ as $\varepsilon \rightarrow 0$, with

$$\|p_\varepsilon(\mathbf{x}, \mathbf{y}, t) - p_0(\mathbf{x}, \mathbf{y}, t)\|_1 \leq c(T)\varepsilon^{\frac{1}{n-1}}, \quad \text{for } 0 \leq t \leq T, \quad \text{as } \varepsilon \rightarrow 0, \quad (34)$$

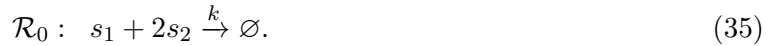
where $c(T)$ is constant independent of ε .

Proof. See Appendix C. □

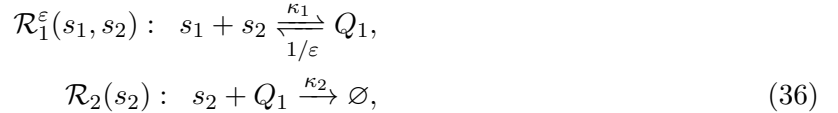
Note that the order of convergence predicted by equation (34), given by $1/(n-1)$, decreases as the order of the input network (28) increases. Generally, note also that the convergence order depends on the kinetic condition (32), i.e. it depends on how the rate coefficients κ_i are scaled, but is independent of the stoichiometric conditions (31).

The family of output networks (29)–(30), parametrized by the stoichiometric coefficients $\{\tilde{\nu}_l\}_{l=1}^m$ and $\tilde{\gamma}_{n-2}$, is not a unique approximation of the input network (28) with a second-order network, i.e. the ordering of the reactants and reactions in (29)–(30) is not unique.

Example 3.1. Consider the third-order input reaction



Under the conditions of Theorem 3.1, reaction (35) may be approximated according to (29)–(30) with an output network $\mathcal{R}_\varepsilon = \mathcal{R}_1^\varepsilon(s_1, s_2) \cup \mathcal{R}_2(s_2)$, with the sub-networks



i.e. the forward reaction from $\mathcal{R}_1^\varepsilon$ is a heteroreaction, involving the distinct reactants s_1 and s_2 . However, the second-order output network $\mathcal{R}_1^\varepsilon(s_2, s_2) \cup \mathcal{R}_2(s_1)$, given by



for which the forward reaction from $\mathcal{R}_1^\varepsilon$ is a homoreaction, also approximates the input reaction (35) under the conditions of Theorem 3.1, which is readily proved analogously as in Appendix B. \triangle

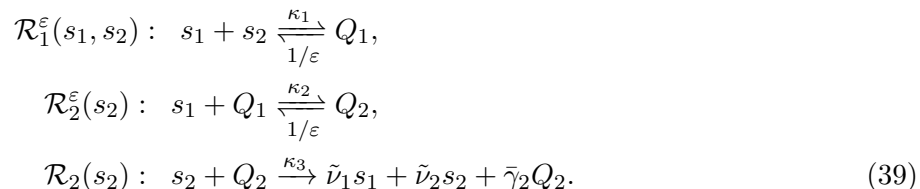
In order to facilitate the proof of Theorem 3.1 in Appendix B, we have followed the convention of ordering the reactants in the input reaction (28) according to increasing stoichiometric coefficients, and we have also fixed the ordering of reactants and reactions in the output networks (29)–(30). For example, if the input reaction is $2s_1 + s_2 \rightarrow \emptyset$, we would re-label the species to obtain $s_1 + 2s_2 \rightarrow \emptyset$. In what follows, we are no longer concerned with proving Theorem 3.1 and, to gain a greater flexibility, we allow arbitrary orderings, and use both of the designs (36) and (37), depending on convenience.

Let us now interpret conditions (31) and (32) from Theorem 3.1. The kinetic condition (32) simply states that the product of the rate coefficients of all of the $(n-1)$ forward (slower) reactions from the output network (30), $\kappa_1\kappa_2 \dots \kappa_{n-1}$, divided by the product of all of the $(n-2)$ backward (faster) reactions, $(1/\varepsilon)^{n-2}$, must be equal to the rate coefficient of the input reaction (28). Furthermore, the asymptotic conditions $\{\varepsilon\kappa_i\}_{i=1}^{n-1} \ll 1$ state that we require the forward reactions to be slower than the backward ones, ensuring validity of the perturbation analysis. The stoichiometric condition (31) also has an intuitive interpretation, as we now exemplify.

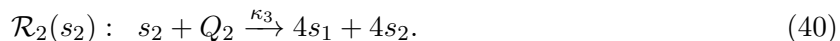
Example 3.2. Consider the fourth-order input reaction



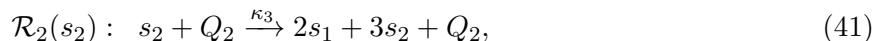
where, using the notation from Theorem 3.1, $\nu_1 = \nu_2 = 2$ and $\bar{\nu}_1 = \bar{\nu}_2 = 4$. A suitable family of output networks is given by $\mathcal{R}_\varepsilon = \mathcal{R}_1^\varepsilon(s_1, s_2) \cup \mathcal{R}_2^\varepsilon(s_1) \cup \mathcal{R}_3(s_2)$, with



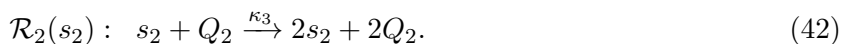
If $\bar{\gamma}_2 = 0$, then (31) implies that $\tilde{\nu}_1 = \tilde{\nu}_2 = 4$, i.e. that $\mathcal{R}_2(s_2)$ from (39) has the same products as the input network (38),



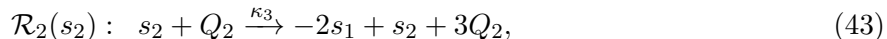
When $0 < \varepsilon \ll 1$, intuitively speaking, at the network level, we formally have $Q_1 = s_1 + s_2$ and $Q_2 = s_1 + Q_1 = 2s_1 + s_2$. With this notation, condition (31) states that we may add the complex $\emptyset = (Q_2 - 2s_1 - s_2)$ to the products of $\mathcal{R}_2(s_2)$ from (39) as many times as desired, as long as the resulting complex contains nonnegative stoichiometric coefficients (so that reaction $\mathcal{R}_2(s_2)$ retains a chemical interpretation). By adding the product complex $\emptyset = (Q_2 - 2s_1 - s_2)$ once to (40), one obtains



while by adding it twice, one gets



Each of the three members (40)–(42) of the family of output networks (39) is valid. However, note that adding the product complex $\emptyset = (Q_2 - 2s_1 - s_2)$ three times to (40) leads to



for which the product complex is not nonnegative: the reaction is non-chemical, and hence not a valid approximation of the input network (38). \triangle

In the remainder of this section, we introduce two more examples. In Section 3.1, we provide an example highlighting how the rate coefficients $\{\kappa_i\}_{i=1}^{n-1}$ from (30) may be chosen in order for the underlying perturbation results to be valid at larger values of ε . In Section 3.2, we illustrate how Theorem 3.1 can be efficiently applied to multi-input networks, i.e. to input networks containing multiple higher-order reactions.

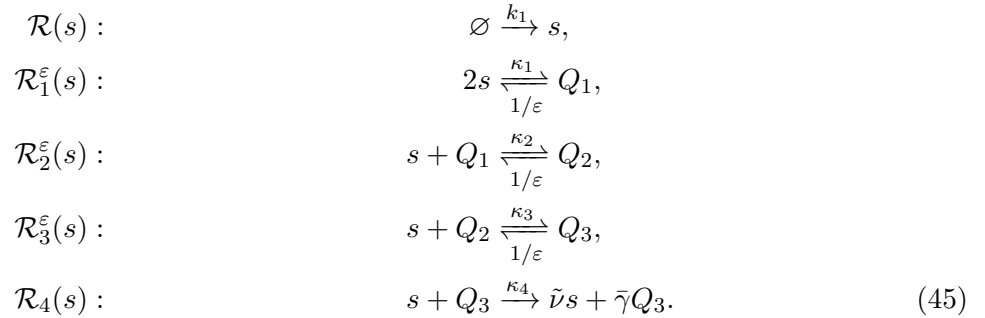
3.1 Example: Chemical Kronecker-delta

Let us consider the fifth-order input reaction network given by



where we fix the dimensionless parameters to $k_1 = k_2 = 1$, and denote the copy-number of species s by x . The stationary PMF of (44) is shown in Figure 3(a) as the black dots, which are interpolated with the solid black lines. The PMF is approximately the Kronecker-delta function that peaks at $x = 4$, which may also be seen directly from the reaction network (44): when the copy-number of species s satisfies $x \leq 4$, only the first reaction may fire, producing x at a constant rate k_1 , i.e. x experiences a constant positive drift until it reaches $x = 5$. On the other hand, when $x \geq 5$, both reactions from (44) may fire. However, owing to the (increasingly) large values of the propensity function of the second reaction from (44) at the states $x \geq 5$, the second reaction overpowers the first one. Thus, x experiences an increasingly net-negative drift for $x \geq 5$. The combined effect of the two reactions from (44) forces the species s to spend most of the time at the single state $x = 4$.

Applying the order-reduction Theorem 3.1, let us approximate the fifth-order input network (44) with the second-order output network $\mathcal{R}_\varepsilon = \mathcal{R} \cup (\cup_{i=1}^3 \mathcal{R}_i^\varepsilon) \cup \mathcal{R}_4$, given by



The stoichiometric condition (31) becomes $\tilde{\nu} = (4 - 4\bar{\gamma})$, and there are two options: $(\tilde{\nu}, \bar{\gamma}) = (4, 0)$, and $(\tilde{\nu}, \bar{\gamma}) = (0, 1)$. In what follows, we arbitrarily take $(\tilde{\nu}, \bar{\gamma}) = (0, 1)$, and denote the copy-number of species s by x , while of species Q_i by y_i , for $i \in \{1, 2, 3\}$.

Having met the stoichiometric condition, it remains to also satisfy the kinetic condition (32). In particular, the rate coefficients from (45) must satisfy:

$$\varepsilon^3 \kappa_1 \kappa_2 \kappa_3 \kappa_4 = k_2, \quad \varepsilon \kappa_i \ll 1, \quad i \in \{1, 2, 3, 4\}, \quad \text{for } 0 < \varepsilon \ll 1. \tag{46}$$

A particular choice of the rate coefficients is given by (33) from Theorem 3.2 with $n = 5$: $\kappa_i = \varepsilon^{-3/4} (k_2)^{1/4}$, for $i \in \{1, 2, 3, 4\}$. While such a simple choice of the rate coefficients is valid, ensuring convergence of order 1/4 for sufficiently small $0 < \varepsilon \ll 1$, it may take very small values of ε for the validity of the underlying perturbation analysis. Let us now discuss how the rate coefficients $\{\kappa_i\}_{i=1}^4$ may be chosen, so that the perturbation analysis is valid already at larger values of ε .

The perturbation analysis employed in this paper relies on scaling the rate coefficients of reactions. A more detailed analysis would consider the whole propensity functions of the reactions. While we do not pursue such an analysis in this paper, let us make a remark. The output network (45) consists of an ordered chain of reactions: in order for the sub-network \mathcal{R}_4 from (45) to fire, and mimic the action of reaction $5s \rightarrow 4s$ from (44), one first requires that the forward reactions in the sub-networks $\mathcal{R}_1^\varepsilon$, $\mathcal{R}_2^\varepsilon$ and $\mathcal{R}_3^\varepsilon$ fire. The reactant complex of the forward reaction from $\mathcal{R}_1^\varepsilon$, forming the start of the chain, is given by $2s$, while the propensity function is $\alpha_1(x) = \kappa_1 x(x-1)$. On the other hand, the forward reactions from $\mathcal{R}_2^\varepsilon$ and $\mathcal{R}_3^\varepsilon$, and the reaction \mathcal{R}_4 , involve the short-lived low-copy-number intermediates Q_1 , Q_2 and Q_3 as reactants, with the propensity functions $\alpha_2(x, y_1) = \kappa_2 x y_1$, $\alpha_3(x, y_2) = \kappa_3 x y_2$ and $\alpha_4(x, y_3) = \kappa_4 x y_3$, respectively. If the induced stochastic dynamics predominantly take place near the x -axis and sufficiently far from the origin (i.e. for lower values of y_1, y_2, y_3 , and higher values of x), then one may observe that $\alpha_i(x, y_i)/\kappa_i \ll \alpha_1(x)/\kappa_1$, for $i \in \{2, 3, 4\}$. In such settings, in order to speed up the slower forward reactions from $\mathcal{R}_2^\varepsilon$ and

$\mathcal{R}_3^\varepsilon$, and the reaction \mathcal{R}_4 , a more efficient choice of the rate coefficients involves larger values of κ_2 , κ_3 and κ_4 , and, due to the constraint (32), smaller values of κ_1 . However, this should be balanced with the fact that, by taking a smaller κ_1 , the chain of reactions from (45) is triggered less often.

Going back to equation (46), let us then choose the rate coefficients e.g. as follows

$$\begin{aligned}\kappa_1 &= \left(\varepsilon^{-3/4}(k_2)^{1/4}\right) \varepsilon^{3\alpha}, \\ \kappa_i &= \left(\varepsilon^{-3/4}(k_2)^{1/4}\right) \varepsilon^{-\alpha}, \quad i \in \{2, 3, 4\}, \quad 0 \leq \alpha < 1/4,\end{aligned}\quad (47)$$

where the condition on the corrective factor α , namely $0 \leq \alpha < 1/4$, ensures that $\{\varepsilon\kappa_i\}_{i=2}^4 \ll 1$ as $\varepsilon \rightarrow 0$. Fixing e.g. $\alpha = 1/8$, in Figure 3(a) we display the stationary x -marginal PMF of the output network (45) for $\varepsilon = 10^{-6}$ as the blue histogram, which is in an excellent agreement with the PMF of the input network (44), shown in black.

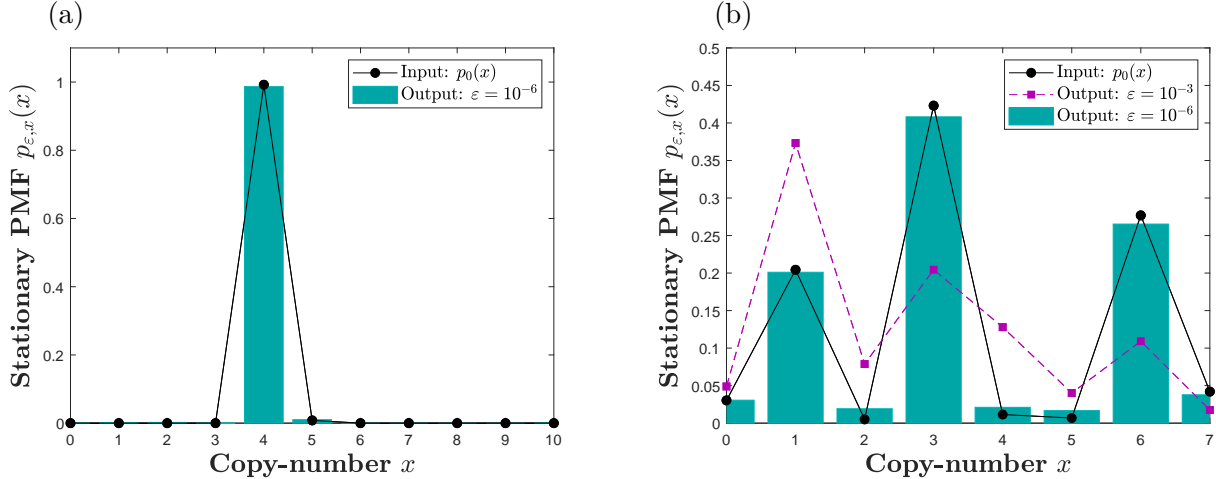


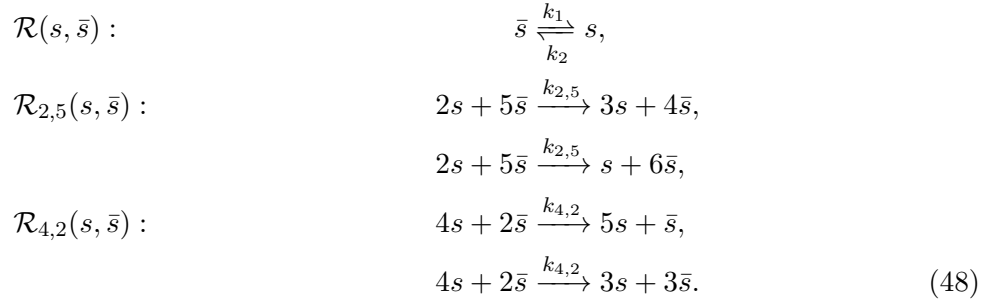
Figure 3: Panel (a) displays the stationary PMF of the fifth-order input network (44) as the black dots, interpolated with the black lines, while the the x -marginal PMF of the second-order output network (45) with $\varepsilon = 10^{-6}$ is shown as the blue histogram. The rest of the dimensionless parameters are fixed to: $k_1 = k_2 = 1$, while $\{\kappa_i\}_{i=1}^4$ are given by (47), with $\alpha = 1/8$. Similarly, panel (b) displays the stationary PMF of the input network (48) in black, while the x -marginal PMF of the output network $\mathcal{R}_\varepsilon = \mathcal{R} \cup (\cup_{i=1}^5 \mathcal{R}_i^\varepsilon \cup \mathcal{R}_4^\varepsilon) \cup \mathcal{R}_6 \cup \mathcal{R}_5$, with the sub-networks given by (49)–(50), as the dashed purple curve when the asymptotic parameter is fixed to $\varepsilon = 10^{-3}$, and as the blue histogram when $\varepsilon = 10^{-6}$. The rest of the dimensionless parameters are fixed to: $k_1 = k_2 = k_{2,5} = k_{4,2} = 1$, while $\{\kappa_i\}_{i=1}^6$, and $\bar{\kappa}_1, \bar{\kappa}_2$ are chosen according to (52), with $\alpha = 1/12$. The conservation constant for the input network is fixed to $c = 7$, and the initial conditions for all of the auxiliary species from the output network, $\{Q_i\}_{i=1}^5, \bar{Q}_4$ are fixed to 0.

3.2 Example: Noise-induced trimodality

Theorem 3.1 provides conditions under which a single higher-order input reaction (28) may be approximated by a second-order network (29)–(30). A generalization to the case of an input network containing multiple higher-order reactions is straightforward: Theorem 3.1 may be applied iteratively to each desired (higher-order) input reaction, one at a time, while the other input reactions, which one does not wish to approximate, are copied directly from the input to the output network without any modifications. Furthermore, if some of the input reactions involve common

reactant sub-complexes, then some of the intermediate species Q_i may be re-used to simultaneously approximate such reactions. Put it another way, reactions with common sub-complexes may be approximated by multiple chains of reactions of the form (30), which all branch out from a suitable common sub-chain. These statements can be readily proved as in Appendix B, under straightforward modifications of the coordinate transformations (57)–(58).

Let us now illustrate an iterative application of Theorem 3.1, and show how the intermediates may be re-used in order to reduce the number of auxiliary species and reactions in the output networks. To this end, consider the seventh-order input reaction network $\mathcal{R}_0 = \mathcal{R} \cup \mathcal{R}_{2,5} \cup \mathcal{R}_{4,2}$, given by



In what follows, we fix the dimensionless parameters to $k_1 = k_2 = k_{2,5} = k_{4,2} = 1$. Denoting the copy-numbers of species s and \bar{s} by x and \bar{x} , respectively, note that their sum is conserved: $x + \bar{x} = c$. In what follows, we fix the conservation constant to $c = 7$. Reaction network (48) has been obtained by applying the so-called noise-control algorithm [9] on the network $\mathcal{R}(s, \bar{s})$, in order to control its stochastic dynamics. Here, sub-networks $\mathcal{R}_{2,5}$ and $\mathcal{R}_{4,2}$, called the zero-drift networks, introduce a state-dependent noise at $x = 2$ and $x \in \{4, 5\}$, respectively, thereby decreasing the PMF at those states, while preserving the mean of the PMF. In Figure 3(b), we display the stationary PMF underlying (48) as the black dots, which are interpolated with the solid black lines for visual clarity. One can notice that the network displays noise-induced trimodality, which is not observed at the deterministic level, where network (48) is monostable, displaying a globally stable equilibrium $x^* = k_1/(k_1 + k_2)c = 3.5$. Let us now apply Theorem 3.1 on the network (48) in order to reduce its order to two, thereby demonstrating that the noise-control algorithm may be useful for molecular computing, where one typically experimentally implements up-to second-order reactions [6].

Applying Theorem 3.1 to independently reduce the order of each of the four reactions underlying $\mathcal{R}_{2,5} \cup \mathcal{R}_{4,2}$ requires 18 auxiliary species and 40 reactions in total, i.e. 10 independent auxiliary species for the network $\mathcal{R}_{2,5}$ (5 species for each of the underlying reactions) and, similarly, 8 species for $\mathcal{R}_{4,2}$. However, 5 auxiliary species are in fact sufficient to reduce the order of network $\mathcal{R}_{2,5}$, since each of the two underlying reactions involve the same reactants, so that we may re-use the auxiliary species. Similar reasoning implies that we require only 4 auxiliary species to approximate the network $\mathcal{R}_{4,2}$. Hence, 9 auxiliary species are sufficient to approximate $\mathcal{R}_{2,5} \cup \mathcal{R}_{4,2}$ by a second-order network. Furthermore, all of the reactions from $\mathcal{R}_{2,5} \cup \mathcal{R}_{4,2}$ involve a common reactant sub-complex $(2s + 2\bar{s})$, i.e. they involve at least 2 molecules of s , and 2 of \bar{s} , which we may further exploit to reduce the number of the auxiliary species. In particular, since $(2s + 2\bar{s})$ may be converted into an auxiliary species in three steps, we may re-use 3 species in both networks $\mathcal{R}_{2,5}$ and $\mathcal{R}_{4,2}$, hence requiring in total 6 auxiliary species. More precisely, sub-network $\mathcal{R}_{2,5}$ may be approximated

by

$$\begin{aligned}
\mathcal{R}_1^\varepsilon(s) &: & 2s \xrightarrow[1/\varepsilon]{\kappa_1} Q_1, \\
\mathcal{R}_2^\varepsilon(\bar{s}) &: & \bar{s} + Q_1 \xrightarrow[1/\varepsilon]{\kappa_2} Q_2, \\
\mathcal{R}_3^\varepsilon(\bar{s}) &: & \bar{s} + Q_2 \xrightarrow[1/\varepsilon]{\kappa_3} Q_3, \\
\mathcal{R}_4^\varepsilon(\bar{s}) &: & \bar{s} + Q_3 \xrightarrow[1/\varepsilon]{\kappa_4} Q_4, \\
\mathcal{R}_5^\varepsilon(\bar{s}) &: & \bar{s} + Q_4 \xrightarrow[1/\varepsilon]{\kappa_5} Q_5, \\
\mathcal{R}_6(s, \bar{s}) &: & \bar{s} + Q_5 \xrightarrow{\kappa_6} 3s + 4\bar{s}, \\
& & \bar{s} + Q_5 \xrightarrow{\kappa_6} s + 6\bar{s},
\end{aligned} \tag{49}$$

and we may re-use the species Q_3 from (49), formally satisfying $Q_3 = (2s + 2\bar{s})$, to make the approximation of the sub-network $\mathcal{R}_{4,2}$ more efficient, as follows:

$$\begin{aligned}
\bar{\mathcal{R}}_4^\varepsilon(s) &: & s + Q_3 \xrightarrow[1/\varepsilon]{\bar{\kappa}_4} \bar{Q}_4, \\
\bar{\mathcal{R}}_5(s, \bar{s}) &: & s + \bar{Q}_4 \xrightarrow{\bar{\kappa}_5} 5s + \bar{s}, \\
& & s + \bar{Q}_4 \xrightarrow{\bar{\kappa}_5} 3s + 3\bar{s}.
\end{aligned} \tag{50}$$

In summary, we have approximated the seventh-order input reaction network $\mathcal{R}_0 = \mathcal{R} \cup \mathcal{R}_{2,5} \cup \mathcal{R}_{4,2}$, given by (48), involving 2 species and 6 reactions, with the second-order output network $\mathcal{R}_\varepsilon \equiv \mathcal{R} \cup (\cup_{i=1}^5 \mathcal{R}_i^\varepsilon \cup \bar{\mathcal{R}}_4^\varepsilon) \cup \mathcal{R}_6 \cup \bar{\mathcal{R}}_5$, involving 8 species and 18 reactions. The sub-network $\mathcal{R}_{2,5}$ from (48) is approximated by $\cup_{i=1}^5 \mathcal{R}_i^\varepsilon \cup \mathcal{R}_6$, while $\mathcal{R}_{4,2}$ by $\cup_{i=1}^3 \mathcal{R}_i^\varepsilon \cup \bar{\mathcal{R}}_4^\varepsilon \cup \bar{\mathcal{R}}_5$.

The output network involving sub-networks (49)–(50) satisfies the stoichiometric conditions (31), while the kinetic conditions (32) are given by

$$\begin{aligned}
\varepsilon^5 \kappa_1 \kappa_2 \kappa_3 \kappa_4 \kappa_5 \kappa_6 &= k_{2,5}, \\
\varepsilon^4 \kappa_1 \kappa_2 \kappa_3 \bar{\kappa}_4 \bar{\kappa}_5 &= k_{4,2}, \quad \{\varepsilon \kappa_i\}_{i=1}^6, \varepsilon \bar{\kappa}_4, \varepsilon \bar{\kappa}_5 \ll 1, \quad \text{with } 0 < \varepsilon \ll 1.
\end{aligned} \tag{51}$$

Guided by the discussion in Section 3.1, let us choose the rate coefficients e.g. as follows

$$\begin{aligned}
\kappa_1 &= \left(\varepsilon^{-\frac{5}{6}} (k_{2,5})^{\frac{1}{6}} \right) \varepsilon^{5\alpha}, \\
\kappa_i &= \left(\varepsilon^{-\frac{5}{6}} (k_{2,5})^{\frac{1}{6}} \right) \varepsilon^{-\alpha}, \quad i \in \{2, 3, \dots, 6\}, \quad 0 \leq \alpha < 1/6, \\
\bar{\kappa}_i &= \varepsilon^{-2} (\kappa_1 \kappa_2 \kappa_3)^{-\frac{1}{2}} (k_{4,2})^{\frac{1}{2}}, \quad i \in \{4, 5\}.
\end{aligned} \tag{52}$$

Fixing e.g. $\alpha = 1/12$ in (52), we display in Figure 3(b) the stationary x -marginal PMF of the output network \mathcal{R}_ε , containing sub-networks (49)–(50), for $\varepsilon = 10^{-3}$, and $\varepsilon = 10^{-6}$, as the purple squares, interpolated with the purple dashed lines, and the blue histogram, respectively. Similar to Figure 1(a), when $\varepsilon = 10^{-3}$, the output PMF is qualitatively accurate, capturing the multimodality, but is quantitatively inaccurately distributed. On the other hand, when $\varepsilon = 10^{-6}$, one can notice a good matching with the stationary PMF of the input network (48), which is shown in black.

4 Discussion

In this paper, we have shown that higher-order (high-molecular) input biochemical networks, containing reactions with three or more reactants, may be stochastically approximated with appropriate second-order (bi-molecular) output ones, containing reactions with up-to two reactants. In particular, it is shown that the probability distributions of the input and output networks match over arbitrarily long time-intervals, when appropriate rate coefficients in the output networks are sufficiently large. The approximation relies on a dimension-expansion: a single n th-order input reaction is replaced by an output network consisting of $(2n - 3)$ reactions of up-to second-order, and involving $(n - 2)$ additional auxiliary species. This has been established by applying singular perturbation theory on the underlying chemical master equation (CME), and stated in Theorems 3.1 and 3.2 in Section 3. We have, thereby, generalized the well-known order-reduction algorithm, which has been used for decades at the deterministic level [20, 21, 22, 23, 24], to the stochastic level and arbitrarily high-order.

In particular, in Section 2, we have first established the result in the special setting when the input reaction is of third-order (tri-molecular), and involves identical reactants, stated as Lemma 2.1. We have applied Lemma 2.1 in Section 2.3, by mapping the third-order Schlögl network [13], given by (23) and displaying a bimodal stationary probability mass function (PMF), to an approximating second-order network, given by (24). It has been verified that the stationary PMF of the approximating network matches that of the Schlögl network in an asymptotic limit of the appropriate rate coefficients, see Figure 1. Furthermore, we have demonstrated that the mean switching time between the two PMF maxima is also preserved under applications of Lemma 2.1, and, in Figure 2, we have numerically verified the theoretically predicted convergence order, given in equation (22).

In Section 3, we have presented our main result: Theorem 3.1, which states that input reactions of arbitrarily high-order, given by (28), may be approximated by families of second-order output ones, given by (29)–(30). In particular, in order for the output networks to replicate the stochastic behavior of the input ones, constraints are imposed on the stoichiometry and kinetics of the output networks, given as conditions (31) and (32), respectively. We have also presented Theorem 3.2, which establishes a weak-convergence result for a sub-family of the output networks, with a convergence order that depends only on the kinetics of the output networks, and not the underlying stoichiometry. In Section 3.1, we have applied Theorem 3.1 on the fifth-order reaction network (44), whose probability distribution is approximately a Kronecker-delta function, arising as a result of a discrete state-space and stochastic dynamics. We have mapped the input network (44) to a family of output networks, given by (45), and discussed how the rate coefficients appearing in (45) may be chosen efficiently. It has been verified that the biochemically realistic network (45), consisting of up-to second-order reactions, also displays the approximate Kronecker-delta probability distribution in an asymptotic limit, see Figure 3(a). Finally, in Section 3.2, we have considered the seventh-order input network (48), which has been designed using the so-called noise-control algorithm [9]. The input network displays noise-induced trimodality, and consists of four higher-order reactions. We have highlighted that Theorem 3.1 can be applied iteratively for multi-input reaction networks, i.e. networks involving multiple higher-order reactions. An efficient iterative application of Theorem 3.1 on the input network (48) has been presented, which significantly reduces the number of reactions and auxiliary species in the resulting output network, given by (49)–(50), whose PMF is shown to converge in Figure 3(b). The noise-control algorithm [9], and Theorem 3.1, jointly provide a systematic framework for designing bi-molecular chemical reaction networks, whose stochastic dynamics are controlled in a state-dependent manner, and which may be experimentally realized in nucleic-acid-based synthetic biology [6].

A Background Theory

Notation. Set \mathbb{R} is the space of real numbers, \mathbb{R}_{\geq} the space of nonnegative real numbers, and $\mathbb{R}_{>}$ the space of positive real numbers. Similarly, \mathbb{Z} is the space of integer numbers, \mathbb{Z}_{\geq} the space of nonnegative integer numbers, and $\mathbb{Z}_{>}$ the space of positive integer numbers. Euclidean row-vectors are denoted in boldface, $\mathbf{x} = (x_1, x_2, \dots, x_N) \in \mathbb{R}^N = \mathbb{R}^{1 \times N}$.

Reaction networks. In this paper, we consider reaction networks $\mathcal{R} = \mathcal{R}(s_1, s_2, \dots, s_N)$, firing in unit-volume reactors under mass-action kinetics, involving N reacting species, $\{s_i\}_{i=1}^N = \{s_1, s_2, \dots, s_N\}$, and M reactions given by

$$\mathcal{R}(s_1, s_2, \dots, s_N) : \sum_{i=1}^N \nu_{ji} s_i \xrightarrow{k_j} \sum_{i=1}^N \bar{\nu}_{ji} s_i, \quad j \in \{1, 2, \dots, M\}. \quad (53)$$

Here, the non-negative linear combinations of the species $\sum_{i=1}^N \nu_{ji} s_i$ and $\sum_{i=1}^N \bar{\nu}_{ji} s_i$ are called the *reactant complex* and the *product complex* of the j -th reaction, respectively, $\boldsymbol{\nu}_j = (\nu_{j1}, \nu_{j2}, \dots, \nu_{jN}) \in \mathbb{Z}_{\geq}^N$ and $\bar{\boldsymbol{\nu}}_j = (\bar{\nu}_{j1}, \bar{\nu}_{j2}, \dots, \bar{\nu}_{jN}) \in \mathbb{Z}_{\geq}^N$ are the corresponding reactant and product stoichiometric vectors, respectively, while $k_j \in \mathbb{R}_{\geq}$ is the *rate coefficient* of the j -th reaction [1, 36]. Abusing the notation slightly, we denote the complex $\sum_{i=1}^N \nu_{ji} s_i$ by $\boldsymbol{\nu}_j$, and reaction $(\sum_{i=1}^N \nu_{ji} s_i \rightarrow \sum_{i=1}^N \bar{\nu}_{ji} s_i) \in \mathcal{R}$ by $(\boldsymbol{\nu}_j \rightarrow \bar{\boldsymbol{\nu}}_j) \in \mathbb{R}$, when convenient. The *order of reaction* $(\boldsymbol{\nu}_j \rightarrow \bar{\boldsymbol{\nu}}_j) \in \mathbb{R}$ is given by $\boldsymbol{\nu}_j \cdot \mathbf{1} < \infty$, where $\mathbf{1} = (1, 1, \dots, 1) \in \mathbb{Z}^N$, and \cdot denotes the vector dot-product. The *order of reaction network* \mathcal{R} is given by the order of its highest-order reaction.

The stochastic model. Let us now consider reaction networks firing in well-mixed reactors, with discrete species counts, and stochastic dynamics. A suitable stochastic description models the time-evolution of species copy-number vector $\mathbf{X}(t) = (X_1(t), \dots, X_N(t)) \in \mathbb{Z}_{\geq}^N$ as a continuous-time discrete-space Markov chain [29], where $t \in \mathbb{R}_{\geq}$ is the time-variable. The underlying probability mass function (PMF) satisfies the partial difference-differential equation, called the *chemical master equation* (CME) [37, 38], given by

$$\frac{\partial}{\partial t} p(\mathbf{x}, t) = \mathcal{L} p(\mathbf{x}, t) = \sum_{j=1}^M (E_{\mathbf{x}}^{-\Delta \mathbf{x}_j} - 1) (\alpha_j(\mathbf{x}) p(\mathbf{x}, t)), \quad (54)$$

where $p(\mathbf{x}, t)$ is the PMF, i.e. the probability that the copy-number vector $\mathbf{X} = \mathbf{X}(t) \in \mathbb{Z}_{\geq}^N$ at time $t > 0$ is given by $\mathbf{x} \in \mathbb{Z}_{\geq}^N$. Here, the linear operator \mathcal{L} is called the *forward operator*, while the *step operator* $E_{\mathbf{x}}^{-\Delta \mathbf{x}} = \prod_{i=1}^N E_{x_i}^{-\Delta x_i}$ is such that $E_{\mathbf{x}}^{-\Delta \mathbf{x}} p(\mathbf{x}, t) = p(\mathbf{x} - \Delta \mathbf{x}, t)$. Vector $\Delta \mathbf{x}_j = (\bar{\nu}_j - \boldsymbol{\nu}_j) \in \mathbb{Z}^N$ is the *reaction vector* of the j -th reaction $(\boldsymbol{\nu}_j \rightarrow \bar{\boldsymbol{\nu}}_j) \in \mathbb{R}$. Function $\alpha_j(\mathbf{x})$ is the propensity (intensity) function of the j -th reaction, and is given by

$$\alpha_j(\mathbf{x}) = k_j \mathbf{x}^{\boldsymbol{\nu}_j} \equiv k_j \prod_{i=1}^N x_i^{\nu_{ji}}, \quad \mathbf{x} \in \mathbb{Z}_{\geq}^N, \quad (55)$$

where $k_j \geq 0$ is the rate coefficient of reaction of the j -th reaction. Here,

$$x_i^{\nu_{ji}} = x_i(x_i - 1)(x_i - 2) \dots (x_i - \nu_{ji} + 1)$$

denotes the ν_{ji} -th factorial power of x_i , with the convention $x_i^0 \equiv 1$ for all $x_i \in \mathbb{Z}_{\geq}$.

Let $\langle p, q \rangle = \sum_{\mathbf{x} \in \mathbb{Z}_{\geq}^N} p(\mathbf{x})q(\mathbf{x})$ denote the l^2 inner-product. The l^2 -adjoint operator of \mathcal{L} , denoted by \mathcal{L}^* and called the *backward operator* [39], is given by

$$\mathcal{L}^*q(\mathbf{x}) = \sum_{j=1}^M \alpha_j(\mathbf{x})(E_{\mathbf{x}}^{+\Delta \mathbf{x}_j} - 1)q(\mathbf{x}). \quad (56)$$

B Proof of Theorem 3.1

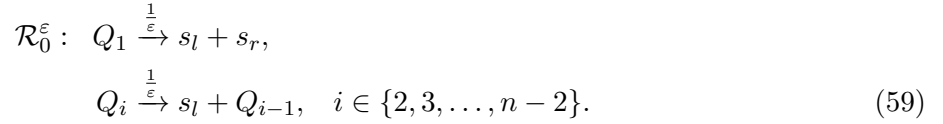
Let $\mathbf{x} = (x_1, \dots, x_m, x_{m+1}, \dots, x_N) \in \mathbb{Z}_{\geq}^N$ be the vector of copy-numbers of the species s_1, \dots, s_N , and $\mathbf{y} = (y_1, \dots, y_{n-2}) \in \mathbb{Z}_{\geq}^{n-2}$ the copy-number vector of the auxiliary species Q_1, \dots, Q_{n-2} from the output network (29)–(30). Let us introduce new variables $\bar{\mathbf{x}} = (\bar{x}_1, \dots, \bar{x}_m, x_{m+1}, \dots, x_N) \in \mathbb{Z}_{\geq}^N$ as follows: if there is only one distinct reactant species in the input network (28), $m = 1$, then

$$\bar{x}_l = \begin{cases} x_1 + \sum_{i=1}^{n-2} (i+1)y_i, & \text{if } l = 1, \\ x_l, & \text{if } l \neq 1. \end{cases} \quad (57)$$

On the other hand, if $m \geq 2$, then

$$\bar{x}_l = \begin{cases} x_1 + \sum_{i=1}^{\nu_1} i y_i + \sum_{i=\nu_1+1}^{n-2} \nu_1 y_i, & \text{if } l = 1, \\ x_2 + \sum_{i=1}^{\nu_1} y_i + \sum_{i=\nu_1+1}^{\nu_1+\nu_2-1} (i - \nu_1 + 1) y_i + \sum_{i=\nu_1+\nu_2}^{n-2} \nu_2 y_i, & \text{if } l = 2, \text{ and } m \neq 2, \\ x_l + \sum_{i=\sum_{j=1}^{l-1} \nu_j}^{\sum_{j=1}^l \nu_j - 1} (i - \sum_{j=1}^{l-1} \nu_j + 1) y_i + \sum_{i=\sum_{j=1}^l \nu_j}^{n-2} \nu_l y_i, & \text{if } l \in \{3, 4, \dots, m-1\}, \\ x_m + \delta_{m,2} \sum_{i=1}^{\nu_1} y_i + \sum_{i=\sum_{j=1}^{m-1} \nu_j + \delta_{m,2}}^{n-2} (i - \sum_{j=1}^{m-1} \nu_j + 1) y_i, & \text{if } l = m. \end{cases} \quad (58)$$

In what follows, for mathematical convenience, we define the fast network



The CME corresponding to (29)–(30), rescaled in time according to $t = \tau/\varepsilon^{n-2}$, and expressed in terms of the new variables $\bar{\mathbf{x}}$, is given by

$$\frac{\partial}{\partial \tau} p_\varepsilon(\bar{\mathbf{x}}, \mathbf{y}, \tau) = \left(\frac{1}{\varepsilon^{n-1}} \mathcal{L}_0 + \frac{1}{\varepsilon^{n-2}} \mathcal{L}_1 \right) p_\varepsilon(\bar{\mathbf{x}}, \mathbf{y}, \tau), \quad (60)$$

where \mathcal{L}_0 is the forward operator of network \mathcal{R}_0^1 in the new coordinates, given by

$$\mathcal{L}_0 = \sum_{i=1}^{n-2} \mathcal{L}_0^i, \quad \mathcal{L}_0^i = \left(E_{y_{i-1}}^{-1} E_{y_i}^{+1} - 1 \right) y_i, \quad i \in \{1, 2, \dots, n-2\}, \quad (61)$$

while \mathcal{L}_1 is the forward operator of the slow sub-network $\mathcal{R}_\varepsilon \setminus \mathcal{R}_0^\varepsilon$, and reads

$$\begin{aligned} \mathcal{L}_1 &= \sum_{i=1}^{n-1} \mathcal{L}_1^i, \quad \mathcal{L}_1^i = \left(E_{y_{i-1}}^{+1} E_{y_i}^{-1} - 1 \right) y_{i-1} \alpha_i(\bar{\mathbf{x}}, \mathbf{y}), \quad i \in \{1, 2, \dots, n-2\}, \\ \mathcal{L}_1^{n-1} &= \left(E_{\bar{\mathbf{x}}}^{-\Delta \bar{\mathbf{x}}} E_{y_{n-2}}^{-\Delta y_{n-2}} - 1 \right) y_{n-2} \alpha_{n-1}(\bar{\mathbf{x}}, \mathbf{y}). \end{aligned} \quad (62)$$

Here, we take the convention that $y_0 \equiv 1$, and that the operators $E_{y_0}^{\pm 1}$ are identity operators, denoted $E_{y_0}^{\pm 1} \equiv 1$. Function $y_{i-1}\alpha_i(\bar{\mathbf{x}}, \mathbf{y})$ is the propensity function of the forward reaction in the sub-network $\mathcal{R}_i^\varepsilon$ from (30), expressed in terms of the new variables (57)–(58). Let us note that \mathcal{L}_1^{n-1} is the only operator which acts on the variable $\bar{\mathbf{x}}$, while the rest of the operators act only on \mathbf{y} .

It follows from (30) that $\Delta y_{n-2} = \bar{\gamma}_{n-2} - 1$. On the other hand, the jump size vector $\Delta \bar{\mathbf{x}}$ is obtained by formally applying the difference operator Δ on (58). Since $\Delta y_i = 0$ for $i \neq (n-2)$, one readily obtains

$$\begin{aligned} \Delta \bar{x}_l &= \Delta x_l + (\nu_l - \delta_{l,m}) \Delta y_{n-2} \\ &= (\tilde{\nu}_l - \delta_{l,m}) + (\nu_l - \delta_{l,m})(\bar{\gamma}_{n-2} - 1), \quad l \in \{1, 2, \dots, m\}. \end{aligned} \quad (63)$$

Let us write the solution of (60) as the perturbation series

$$p_\varepsilon(\bar{\mathbf{x}}, \mathbf{y}, \tau) = \sum_{i=0}^{n-1} \varepsilon^i p_i(\bar{\mathbf{x}}, \mathbf{y}, \tau) + \dots \quad (64)$$

Substituting (64) into (60), and equating terms of equal powers in ε , the following system of n equations is obtained:

$$\begin{aligned} \mathcal{O}\left(\frac{1}{\varepsilon^{n-i}}\right) : \mathcal{L}_0 p_{i-1}(\bar{\mathbf{x}}, \mathbf{y}, \tau) &= -\mathcal{L}_1 p_{i-2}(\bar{\mathbf{x}}, \mathbf{y}, \tau), \quad i \in \{1, 2, \dots, n-1\}, \\ \mathcal{O}(1) : \mathcal{L}_0 p_{n-1}(\bar{\mathbf{x}}, \mathbf{y}, \tau) &= \frac{\partial}{\partial \tau} p_0(\bar{\mathbf{x}}, \mathbf{y}, \tau) - \mathcal{L}_1 p_{n-2}(\bar{\mathbf{x}}, \mathbf{y}, \tau), \end{aligned} \quad (65)$$

with the convention that $p_{-1}(\bar{\mathbf{x}}, \mathbf{y}, \tau) \equiv 0$.

Order $1/\varepsilon^{n-1}$ equation. Operator \mathcal{L}_0 , given in (61), acts only on the variable \mathbf{y} , and each summand \mathcal{L}_0^i is multiplied on the right by a factor y_i . It follows that $p_0(\bar{\mathbf{x}}, \mathbf{y}, \tau) = p_0(\mathbf{y}, \tau) p_0(\bar{\mathbf{x}}, \tau)$, so that the equation becomes $\mathcal{L}_0 p_0(\mathbf{y}, \tau) = 0$. Operator \mathcal{L}_0 has a one-dimensional null-space, $\mathcal{N}(\mathcal{L}_0) = \{1_{\mathbf{y}} \prod_{i=1}^{n-2} \delta_{y_i, 0}\}$, where $1_{\mathbf{y}}$ is a function independent of \mathbf{y} . A normalized element of the null-space is given by

$$p_0(\bar{\mathbf{x}}, \mathbf{y}, \tau) = p_0(\bar{\mathbf{x}}, \tau) \prod_{i=1}^{n-2} \delta_{y_i, 0}, \quad \sum_{\bar{\mathbf{x}}} p_0(\bar{\mathbf{x}}, \tau) = 1, \quad \text{for } \tau \geq 0. \quad (66)$$

Order $1/\varepsilon^{n-2}$ equation. Since each summand $\{\mathcal{L}_1^i\}_{i=2}^{n-1}$ from (62) is multiplied on the right by a nonconstant factor y_{i-1} , equation (66) implies

$$\mathcal{L}_1 p_0(\bar{\mathbf{x}}, \mathbf{y}, \tau) = p_0(\bar{\mathbf{x}}, \tau) \prod_{i=2}^{n-2} \delta_{y_i, 0} \mathcal{L}_1^1 \delta_{y_1, 0}. \quad (67)$$

The null-space of the backward operator is given by $\mathcal{N}(\mathcal{L}_0^*) = \{1_{\mathbf{y}}\}$, and the solvability condition is $0 = \langle 1_{\mathbf{y}}, \mathcal{L}_1 p_0(\bar{\mathbf{x}}, \mathbf{y}, \tau) \rangle = \langle (\mathcal{L}_1^1)^* 1_{\mathbf{y}}, p_0(\bar{\mathbf{x}}, \tau) \prod_{i=1}^{n-2} \delta_{y_i, 0} \rangle$, where $(\mathcal{L}_1^1)^* = \alpha_1(\bar{\mathbf{x}}, \mathbf{y})(E_{y_1}^{+1} - 1)$ and $\langle f, g \rangle = \sum_{\mathbf{y}} f(\mathbf{y})g(\mathbf{y})$. Since $(\mathcal{L}_1^1)^* 1_{\mathbf{y}} = 0$, the solvability condition is unconditionally satisfied.

Let us write the solution of the $\mathcal{O}(1/\varepsilon^{n-2})$ equation from (65) in the separable form

$$p_1(\bar{\mathbf{x}}, \mathbf{y}, \tau) = p_0(\bar{\mathbf{x}}, \tau) p_1(y_1; \bar{\mathbf{x}}) \prod_{i=2}^{n-2} \delta_{y_i, 0}. \quad (68)$$

Substituting (68) into the $\mathcal{O}(1/\varepsilon^{n-2})$ equation, using (67) and

$$\mathcal{L}_0 p_1(\bar{\mathbf{x}}, \mathbf{y}, \tau) = p_0(\bar{\mathbf{x}}, \tau) \prod_{i=2}^{n-2} \delta_{y_i,0} \mathcal{L}_0^1 p_1(y_1; \bar{\mathbf{x}}),$$

and the operator equality $(E_{y_1}^{-1} - 1) = -(E_{y_1}^{+1} - 1)E_{y_1}^{-1}$, one obtains

$$\prod_{i=2}^{n-2} \delta_{y_i,0} (E_{y_1}^{+1} - 1) (y_1 p_1(y_1; \bar{\mathbf{x}}) - E_{y_1}^{-1} \alpha_1(\bar{\mathbf{x}}, \mathbf{y}) \delta_{y_1,0}) = 0. \quad (69)$$

Equation (69) is identically satisfied if $(y_2, y_3, \dots, y_{n-2}) \neq \mathbf{0}_{n-3}$, where $\mathbf{0}_n$ is the zero element of \mathbb{Z}_{\geq}^n . On the other hand, if $(y_2, y_3, \dots, y_{n-2}) = \mathbf{0}_{n-3}$, it follows that the solutions satisfy

$$y_1 p_1(y_1; \bar{\mathbf{x}}) = E_{y_1}^{-1} \alpha_1(\bar{\mathbf{x}}, (y_1, \mathbf{0}_{n-3})) \delta_{y_1,0}. \quad (70)$$

Order $1/\varepsilon^{n-3}$ equation. It follows from (62) and (68) that

$$\mathcal{L}_1 p_1(\bar{\mathbf{x}}, \mathbf{y}, \tau) = p_0(\bar{\mathbf{x}}, \tau) \prod_{i=3}^{n-2} \delta_{y_i,0} (\mathcal{L}_1^1 + \mathcal{L}_1^2) p_1(y_1; \bar{\mathbf{x}}) \delta_{y_2,0}, \quad (71)$$

and the solvability condition $0 = \langle \mathbf{1}_{\mathbf{y}}, \mathcal{L}_1 p_1(\bar{\mathbf{x}}, \mathbf{y}, \tau) \rangle$ is unconditionally satisfied, since $(\mathcal{L}_1^1 + \mathcal{L}_1^2)^* \mathbf{1}_{\mathbf{y}} = 0$.

Let us write the solution of the $\mathcal{O}(1/\varepsilon^{n-3})$ equation from (65) in the separable form

$$p_2(\bar{\mathbf{x}}, \mathbf{y}, \tau) = p_0(\bar{\mathbf{x}}, \tau) p_2(y_1, y_2; \bar{\mathbf{x}}) \prod_{i=3}^{n-2} \delta_{y_i,0}. \quad (72)$$

Substituting (72) into the $\mathcal{O}(1/\varepsilon^{n-3})$ equation, using (71) and

$$\mathcal{L}_0 p_2(\bar{\mathbf{x}}, \mathbf{y}, \tau) = p_0(\bar{\mathbf{x}}, \tau) \prod_{i=3}^{n-2} \delta_{y_i,0} (\mathcal{L}_0^1 + \mathcal{L}_0^2) p_2(y_1, y_2; \bar{\mathbf{x}}),$$

and the operator equalities $(E_{y_1}^{-1} - 1) = -(E_{y_1}^{+1} - 1)E_{y_1}^{-1}$, $(E_{y_1}^{+1} E_{y_2}^{-1} - 1) = -(E_{y_1}^{-1} E_{y_2}^{+1} - 1)E_{y_1}^{+1} E_{y_2}^{-1}$, one obtains

$$\begin{aligned} 0 &= \prod_{i=3}^{n-2} \delta_{y_i,0} (E_{y_1}^{+1} - 1) [y_1 p_2(y_1, y_2; \bar{\mathbf{x}}) - E_{y_1}^{-1} \alpha_1(\bar{\mathbf{x}}, \mathbf{y}) \delta_{y_2,0} p_1(y_1; \bar{\mathbf{x}})] \\ &+ \prod_{i=3}^{n-2} \delta_{y_i,0} (E_{y_1}^{-1} E_{y_2}^{+1} - 1) [y_2 p_2(y_1, y_2; \bar{\mathbf{x}}) - E_{y_1}^{+1} E_{y_2}^{-1} \alpha_2(\bar{\mathbf{x}}, \mathbf{y}) \delta_{y_2,0} y_1 p_1(y_1; \bar{\mathbf{x}})]. \end{aligned} \quad (73)$$

Equation (73) is identically satisfied if $(y_3, y_4, \dots, y_{n-2}) \neq \mathbf{0}_{n-4}$. On the other hand, if $(y_3, y_4, \dots, y_{n-2}) = \mathbf{0}_{n-4}$, the solutions satisfy

$$y_1 p_2(y_1, y_2; \bar{\mathbf{x}}) = E_{y_1}^{-1} \alpha_1(\bar{\mathbf{x}}, (y_1, y_2, \mathbf{0}_{n-4})) \delta_{y_2,0} p_1(y_1; \bar{\mathbf{x}}), \quad (74)$$

and

$$\begin{aligned} y_2 p_2(y_1, y_2; \bar{\mathbf{x}}) &= E_{y_1}^{+1} E_{y_2}^{-1} \alpha_2(\bar{\mathbf{x}}, (y_1, y_2, \mathbf{0}_{n-4})) \delta_{y_2,0} (y_1 p_1(y_1; \bar{\mathbf{x}})) \\ &= E_{y_1}^{+1} E_{y_2}^{-1} \alpha_2(\bar{\mathbf{x}}, (y_1, y_2, \mathbf{0}_{n-4})) \delta_{y_2,0} (E_{y_1}^{-1} \alpha_1(\bar{\mathbf{x}}, (y_1, \mathbf{0}_{n-3})) \delta_{y_1,0}) \\ &= \delta_{y_1,0} \alpha_1(\bar{\mathbf{x}}, (y_1, \mathbf{0}_{n-3})) E_{y_1}^{+1} E_{y_2}^{-1} \alpha_2(\bar{\mathbf{x}}, (y_1, y_2, \mathbf{0}_{n-4})) \delta_{y_2,0}, \end{aligned} \quad (75)$$

where we have used (70) when going from the first to the second line in (75).

Order $1/\varepsilon^{n-i}$ equation, $i \in \{3, 4, \dots, n-1\}$. One can inductively proceed to the higher-order equations from (65), with the solutions of the $\mathcal{O}(1/\varepsilon^{n-i})$ equation written in the separable form

$$p_{i-1}(\bar{\mathbf{x}}, \mathbf{z}, t) = p_0(\bar{\mathbf{x}}, t) p_{i-1}(z_1, \dots, z_{i-1}; \bar{\mathbf{x}}) \prod_{j=i}^{n-2} \delta_{z_j, 0}, \quad i \in \{1, 2, \dots, n-1\}, \quad (76)$$

with the convention that $\prod_{i=a}^b f(i) = 1$ if $a > b$, where $f(i)$ is an arbitrary function of i , and $p_0(z_0; \bar{\mathbf{x}}) \equiv 1$ (see also equations (66), (68) and (72)). It can be readily shown that the results (70) and (75) generalize to

$$y_i p_i(y_1, \dots, y_i; \bar{\mathbf{x}}) = \left(\prod_{j=1}^{i-1} \delta_{y_j, 0} E_{y_{j-1}}^{+1} \alpha_j(\bar{\mathbf{x}}, (y_1, \dots, y_j, \mathbf{0}_{n-2-j})) \right) \times E_{y_{i-1}}^{+1} E_{y_i}^{-1} \alpha_i(\bar{\mathbf{x}}, (y_1, \dots, y_i, \mathbf{0}_{n-2-i})) \delta_{y_i, 0}, \quad i \in \{1, 2, \dots, n-2\}. \quad (77)$$

As is shortly shown, the effective CME, at the order one, depends on p_{n-2} only via the product $y_{n-2} p_{n-2}$ satisfying (77); see equation (79).

Order 1 equation. The solvability condition is given by $0 = \langle 1, \partial/\partial\tau p_0(\bar{\mathbf{x}}, \mathbf{y}, \tau) \rangle - \langle 1, \mathcal{L}_1 p_{n-2}(\bar{\mathbf{x}}, \mathbf{y}, \tau) \rangle$. Equation (66) implies $\langle 1, \partial/\partial\tau p_0(\bar{\mathbf{x}}, \mathbf{y}, \tau) \rangle = \frac{\partial}{\partial\tau} p_0(\bar{\mathbf{x}}, \tau)$. On the other hand, equation (62), and the fact that $(\sum_{i=1}^{n-2} \mathcal{L}_1^i)^* 1 = 0$, imply that $\langle 1, \mathcal{L}_1 p_{n-2}(\bar{\mathbf{x}}, \mathbf{y}, \tau) \rangle = \langle 1, \mathcal{L}_1^{n-1} p_{n-2}(\bar{\mathbf{x}}, \mathbf{y}, \tau) \rangle$, so that the solvability condition becomes

$$\frac{\partial}{\partial\tau} p_0(\bar{\mathbf{x}}, \tau) = \langle 1, \mathcal{L}_1^{n-1} p_{n-2}(\bar{\mathbf{x}}, \mathbf{y}, \tau) \rangle. \quad (78)$$

Let us simplify the RHS from (78):

$$\begin{aligned} \langle 1, \mathcal{L}_1^{n-1} p_{n-2}(\bar{\mathbf{x}}, \mathbf{y}, \tau) \rangle &= \langle 1, \left(E_{\bar{\mathbf{x}}}^{-\Delta\bar{\mathbf{x}}} E_{y_{n-2}}^{-\Delta y_{n-2}} - 1 \right) \alpha_{n-1}(\bar{\mathbf{x}}, \mathbf{y}) y_{n-2} p_{n-2}(\bar{\mathbf{x}}, \mathbf{y}, \tau) \rangle \\ &= \langle E_{y_{n-2}}^{+\Delta y_{n-2}} 1, E_{\bar{\mathbf{x}}}^{-\Delta\bar{\mathbf{x}}} \alpha_{n-1}(\bar{\mathbf{x}}, \mathbf{y}) y_{n-2} p_{n-2}(\bar{\mathbf{x}}, \mathbf{y}, \tau) \rangle \\ &\quad - \langle 1, \alpha_{n-1}(\bar{\mathbf{x}}, \mathbf{y}) y_{n-2} p_{n-2}(\bar{\mathbf{x}}, \mathbf{y}, \tau) \rangle \\ &= \langle 1, \left(E_{\bar{\mathbf{x}}}^{-\Delta\bar{\mathbf{x}}} - 1 \right) \alpha_{n-1}(\bar{\mathbf{x}}, \mathbf{y}) y_{n-2} p_{n-2}(\bar{\mathbf{x}}, \mathbf{y}, \tau) \rangle \\ &= \left(E_{\bar{\mathbf{x}}}^{-\Delta\bar{\mathbf{x}}} - 1 \right) p_0(\bar{\mathbf{x}}, \tau) \langle 1, \alpha_{n-1}(\bar{\mathbf{x}}, \mathbf{y}) y_{n-2} p_{n-2}(\mathbf{y}; \bar{\mathbf{x}}) \rangle \end{aligned} \quad (79)$$

where, when going to the last line, we use $p_{n-2}(\bar{\mathbf{x}}, \mathbf{y}, \tau) = p_0(\bar{\mathbf{x}}, \tau) p_{n-2}(\mathbf{y}; \bar{\mathbf{x}})$. Hence, the effective

CME depends on the p_{n-2} only via the product $y_{n-2}p_{n-2}$. Using (77) with $i = n - 2$, one obtains

$$\begin{aligned}
\langle 1, \alpha_{n-1}(\bar{\mathbf{x}}, \mathbf{y}) y_{n-2} p_{n-2}(\mathbf{y}; \bar{\mathbf{x}}) \rangle &= \langle \alpha_{n-1}(\bar{\mathbf{x}}, \mathbf{y}) \left(\prod_{j=1}^{n-3} \delta_{y_j, 0} E_{y_{j-1}}^{+1} \alpha_j(\bar{\mathbf{x}}, (y_1, \dots, y_j, \mathbf{0}_{n-2-j})) \right), \\
&\quad E_{y_{n-3}}^{+1} E_{y_{n-2}}^{-1} \alpha_{n-2}(\bar{\mathbf{x}}, \mathbf{y}) \delta_{y_{n-2}, 0} \rangle \\
&= \langle E_{y_{n-2}}^{+1} \alpha_{n-1}(\bar{\mathbf{x}}, \mathbf{y}) \left(\prod_{j=1}^{n-3} \delta_{y_j, 0} E_{y_{j-1}}^{+1} \alpha_j(\bar{\mathbf{x}}, (y_1, \dots, y_j, \mathbf{0}_{n-2-j})) \right), \\
&\quad E_{y_{n-3}}^{+1} \alpha_{n-2}(\bar{\mathbf{x}}, \mathbf{y}) \delta_{y_{n-2}, 0} \rangle \\
&= \langle 1, \left(\prod_{j=1}^{n-2} \delta_{y_j, 0} \right) \left(\prod_{j=1}^{n-3} E_{y_{j-1}}^{+1} \alpha_j(\bar{\mathbf{x}}, (y_1, \dots, y_j, \mathbf{0}_{n-2-j})) \right) \rangle \\
&= \langle E_{y_{n-3}}^{+1} \alpha_{n-2}(\bar{\mathbf{x}}, \mathbf{y}) \left(E_{y_{n-2}}^{+1} \alpha_{n-1}(\bar{\mathbf{x}}, \mathbf{y}) \right) \rangle \\
&= \prod_{j=1}^{n-1} \alpha_j(\bar{\mathbf{x}}, (\mathbf{0}_{j-2}, 1, \mathbf{0}_{n-(j+1)})), \tag{80}
\end{aligned}$$

with the convention that $\alpha_1(\bar{\mathbf{x}}, (\mathbf{0}_{-1}, 1, \mathbf{0}_{n-2})) \equiv \alpha_1(\bar{\mathbf{x}}, \mathbf{0}_{n-2})$, $\alpha_2(\bar{\mathbf{x}}, (\mathbf{0}_0, 1, \mathbf{0}_{n-3})) \equiv \alpha_2(\bar{\mathbf{x}}, (1, \mathbf{0}_{n-3}))$, and $\alpha_{n-1}(\bar{\mathbf{x}}, (\mathbf{0}_{n-3}, 1, \mathbf{0}_0)) \equiv \alpha_{n-1}(\bar{\mathbf{x}}, (\mathbf{0}_{n-3}, 1))$. In words, propensity function α_j is evaluated at $y_{j-1} = 1$, and $y_i = 0$ for $i \neq (j - 1)$ in (80).

Now, if $m = 1$, using (57), it follows that $\alpha_1(x_1, \mathbf{0}_{n-2}) = \kappa_1 \bar{x}_1 (\bar{x}_1 - 1)$, and $\alpha_j(\bar{x}_1, (\mathbf{0}_{j-2}, 1, \mathbf{0}_{n-(j+1)})) = \kappa_j (\bar{x}_1 - j)$, for $j \in \{2, 3, \dots, n - 1\}$. Hence, in this case,

$$\prod_{j=1}^{n-1} \alpha_j(\bar{\mathbf{x}}, (\mathbf{0}_{j-2}, 1, \mathbf{0}_{n-(j+1)})) = \left(\prod_{j=1}^{n-1} \kappa_j \right) \bar{x}_1^n, \quad \text{if } m = 1. \tag{81}$$

Similarly, in the case $m \geq 2$, using (58), one obtains

$$\prod_{j=1}^{n-1} \alpha_j(\bar{\mathbf{x}}, (\mathbf{0}_{j-2}, 1, \mathbf{0}_{n-(j+1)})) = \left(\prod_{j=1}^{n-1} \kappa_j \right) \prod_{l=1}^m \bar{x}_l^{\nu_l}, \quad \text{if } m \geq 2. \tag{82}$$

Substituting (79)–(82) into (78), and changing the time back to the original scale, $\tau = \varepsilon^{n-2} t$, one obtains the effective CME

$$\frac{\partial}{\partial t} p_0(\bar{\mathbf{x}}, t) = \left(E_{\bar{\mathbf{x}}}^{-\Delta \bar{\mathbf{x}}} - 1 \right) \left(\varepsilon^{n-2} \prod_{j=1}^{n-1} \kappa_j \right) \prod_{l=1}^m \bar{x}_l^{\nu_l} p_0(\bar{\mathbf{x}}, t). \tag{83}$$

In order for the effective CME (83) to match the CME of the input network (28), we firstly require that the stoichiometric vectors of the input network and the effective output network are the same: $\Delta \bar{x}_l = (\bar{\nu}_l - \nu_l)$, which, using (63), gives the stoichiometric conditions (31). And, secondly, we require that the effective propensity function is equal to the propensity function of the input network, $\alpha_{\text{eff}}(\mathbf{x}) = \varepsilon^{n-2} \prod_{j=1}^{n-1} \kappa_j \prod_{l=1}^m x_l^{\nu_l} = \alpha(\mathbf{x}) = k \prod_{l=1}^m x_l^{\nu_l}$, which results in the kinetic condition (32).

Assuming convergence of the perturbation series (64), it follows from (66) that the time-dependent copy-number vector $\mathbf{Y}(t) \in \mathbb{Z}_{\geq}^{n-2}$ converges weakly (in distribution) to $\mathbf{0} \in \mathbb{Z}_{\geq}^{n-2}$ (a

deterministic variable), and hence it also converges to zero in probability. It then follows from (57)–(58) that $\bar{\mathbf{X}}(t)$ converges to $\mathbf{X}(t)$ in probability as $\varepsilon \rightarrow 0$, and so we may replace $\bar{\mathbf{x}}$ by \mathbf{x} in (83), ensuring that the effective CME tracks copy-numbers of the species s_1, \dots, s_N .

C Proof of Theorem 3.2

Consider the output network (29)–(30), satisfying the kinetic condition (32), with the rate coefficients satisfying (33), whose CME is given by

$$\frac{\partial}{\partial t} p_\varepsilon(\bar{\mathbf{x}}, \mathbf{y}, t) = \left(\frac{1}{\varepsilon} \mathcal{L}_0 + \frac{1}{\varepsilon^{\frac{n-2}{n-1}}} \mathcal{L}_1 \right) p_\varepsilon(\bar{\mathbf{x}}, \mathbf{y}, t). \quad (84)$$

Here, the operators \mathcal{L}_0 and \mathcal{L}_1 have the form as in (61)–(62), and involve rate coefficients which are $\mathcal{O}(1)$ with respect to ε . In what follows, we assume the state-space for (84) is bounded.

Let us write the solution $p_\varepsilon(\bar{\mathbf{x}}, \mathbf{y}, t)$ in the following form:

$$p_\varepsilon(\bar{\mathbf{x}}, \mathbf{y}, t) = \sum_{i=0}^{n-1} \varepsilon^{\frac{i}{n-1}} p_i(\bar{\mathbf{x}}, \mathbf{y}, t) + r_n(\bar{\mathbf{x}}, \mathbf{y}, t), \quad (85)$$

where functions $\{p_i(\bar{\mathbf{x}}, \mathbf{y}, t)\}_{i=1}^{n-1}$ satisfy (65). As shown in Appendix B, there are infinitely many solutions $p_i(\bar{\mathbf{x}}, \mathbf{y}, t)$ for each fixed i (see equations (76)–(77)), and we now chose those that are bounded, with bounded time-derivatives. Substituting (85) into (84), using (65), and writing $p_i(t) = p_i(\bar{\mathbf{x}}, \mathbf{y}, t)$, $r_n(t) = r_n(\bar{\mathbf{x}}, \mathbf{y}, t)$ and $\mathcal{L}_\varepsilon \equiv (\varepsilon^{-1} \mathcal{L}_0 + \varepsilon^{-(n-2)/(n-1)} \mathcal{L}_1)$, one obtains an equation governing the time-evolution of the remainder function $r_n(t)$:

$$\frac{\partial}{\partial t} r_n(t) = \mathcal{L}_\varepsilon r_n(t) + \varepsilon^{\frac{1}{n-1}} \left(\mathcal{L}_1 p_{n-1}(t) - \frac{\partial}{\partial t} p_1(t) \right) + \sum_{i=2}^{n-1} \varepsilon^{\frac{i}{n-1}} \frac{\partial}{\partial t} p_i(t). \quad (86)$$

The solution of the non-homogenous linear ODE (86) may be written as

$$\begin{aligned} r_n(t) &= e^{\mathcal{L}_\varepsilon t} r_n(0) + \varepsilon^{\frac{1}{n-1}} \int_0^t e^{\mathcal{L}_\varepsilon(t-s)} \left(\mathcal{L}_1 p_{n-1}(s) - \frac{\partial}{\partial t} p_1(s) \right) ds \\ &\quad + \sum_{i=2}^{n-1} \varepsilon^{\frac{i}{n-1}} \int_0^t e^{\mathcal{L}_\varepsilon(t-s)} \frac{\partial}{\partial t} p_i(s) ds, \end{aligned} \quad (87)$$

where $r(t)$ and $p_i(t)$ are interpreted here as column vectors on the bounded state-space, and $e^{\mathcal{L}_\varepsilon t}$ is a matrix exponential. Let us assume $p_\varepsilon(0) = p_0(0)$, so that (85) implies an initial condition for the remainder function:

$$r_n(0) = - \sum_{i=1}^{n-1} \varepsilon^{\frac{i}{n-1}} p_i(0). \quad (88)$$

Let $\|\cdot\|_1$ denote the l^1 -norm over the bounded state-spaces of $\bar{\mathbf{x}}$ and \mathbf{y} , as well as the induced matrix-operator norm. Applying the l^1 -norm on (87), using the triangle inequality, and the fact that $\|e^{\mathcal{L}_\varepsilon t}\|_1 = 1$ [39], one obtains

$$\begin{aligned} \|r_n(t)\|_1 &\leq \varepsilon^{\frac{1}{n-1}} \left(\|p_1(0)\|_1 + t \sup_{0 \leq s \leq t} \left\| \mathcal{L}_1 p_{n-1}(s) - \frac{\partial}{\partial t} p_1(s) \right\|_1 \right) \\ &\quad + \sum_{i=2}^{n-1} \varepsilon^{\frac{i}{n-1}} \left(\|p_i(0)\|_1 + t \sup_{0 \leq s \leq t} \left\| \frac{\partial}{\partial t} p_i(s) \right\|_1 \right). \end{aligned} \quad (89)$$

Since $p_i(t)$ are chosen to be bounded, with bounded time-derivatives, it follows that the remainder $r_n(t) \rightarrow 0$ as $\varepsilon \rightarrow 0$ for any fixed $t > 0$. It then follows from (85) that $p_\varepsilon \rightarrow p_0$ as $\varepsilon \rightarrow 0$. Since $p_0(\bar{\mathbf{x}}, \mathbf{y}, t) = p_0(\bar{\mathbf{x}}, t) \prod_{i=1}^{n-2} \delta_{y_i, 0}$ (see equation (66)), it follows that the auxiliary species converge to zero, $\mathbf{Z}(t) \rightarrow \mathbf{0}$, and equations (57)–(58) imply $\bar{\mathbf{X}}(t) \rightarrow \mathbf{X}(t)$. For sufficiently small ε , the remainder is asymptotically given by $\|r_n(t)\|_1 = \mathcal{O}(\varepsilon^{\frac{1}{n-1}})$, so that (85) implies (34).

References

- [1] Feinberg, M. *Lectures on chemical reaction networks*. Delivered at the Mathematics Research Center, University of Wisconsin, 1979.
- [2] Érdi, P., Tóth, J. *Mathematical models of chemical reactions. Theory and applications of deterministic and stochastic Models*. Manchester University Press, Princeton University Press, 1989.
- [3] Vilar, J. M. G., Kueh, H. Y., Barkai, N., Leibler, S., 2002. Mechanisms of noise-resistance in genetic oscillators. *Proceedings of the National Academy of Sciences of the United States of America*, **99**(9): 5988–5992.
- [4] Dublanche, Y., Michalodimitrakis, K., Kummerer, N., Foglierini, M., Serrano, L., 2006. Noise in transcription negative feedback loops: simulation and experimental analysis. *Molecular Systems Biology*, **2**(41): E1–E12.
- [5] Kar, S., Baumann, W. T., Paul M. R. and Tyson, J. J., 2009. Exploring the roles of noise in the eukaryotic cell cycle. *Proceedings of the National Academy of Sciences of USA*, **106**: 6471–6476.
- [6] Soloveichik, D., Seeling, G., Winfree, E., 2010. DNA as a universal substrate for chemical kinetics. *Proceedings of the National Academy of Sciences*, **107**(12): 5393–5398.
- [7] Soloveichik, D., Cook, M., Winfree, E., Bruck, J., 2008. Computation with finite stochastic chemical reaction networks. *Natural Computing*, **7**(4): 615–633.
- [8] Plesa, T., Vejchodský, T., and Erban, R., 2016. Chemical reaction systems with a homoclinic bifurcation: An inverse problem. *Journal of Mathematical Chemistry*, **54**(10): 1884–1915.
- [9] Plesa, T., and Zygalakis, K. C., Anderson, D. F., and Erban, R., 2018. Noise control for molecular computing. *Journal of the Royal Society Interface*, **15**(144): 20180199.
- [10] Srinivas, N., Parkin, J., Seeling, G., Winfree, E., Soloveichik, D., 2017. Enzyme-free nucleic acid dynamical systems. *Science*, **358**, eaal2052.
- [11] Gillespie, D. *Markov processes: An introduction for physical scientists*. Academic Press, Inc., Harcourt Brace Jovanowich, 1992.
- [12] Cardelli L., 2013. Two-domain DNA strand displacement *Math. Struc. in Comp. Science*, **23**: 247–271.
- [13] Schlögl, F., 1972. Chemical reaction models for nonequilibrium phase transition. *Z. Physik.*, **253**(2): 147–161.
- [14] Prigogine, I., and Lefever, R., 1968. Symmetry breaking instabilities in dissipative systems II. *Journal of Chemical Physics*, **48**(4): 1695–1700.

- [15] Schnakenberg, J., 1979. Simple chemical reaction systems with limit cycle behaviour. *Journal of Theoretical Biology*, **81**(3): 389–400.
- [16] Plesa, T., Vejchodský, T., and Erban, R., 2017. Test models for statistical inference: Two-dimensional reaction systems displaying limit cycle bifurcations and bistability, 2017. *Stochastic Dynamical Systems, Multiscale Modeling, Asymptotics and Numerical Methods for Computational Cellular Biology*. Available as <https://arxiv.org/abs/1607.07738>.
- [17] Erban, R., Chapman, S. J., Kevrekidis, I. and Vejchodsky, T., 2009. Analysis of a stochastic chemical system close to a SNIPER bifurcation of its mean-field model. *SIAM Journal on Applied Mathematics*, **70**(3): 984–1016.
- [18] Cao, Y., and Erban, R., 2014. Stochastic Turing patterns: analysis of compartment-based approaches. *Bulletin of Mathematical Biology*, **76**(12): 3051–3069.
- [19] Li, F., Chen, M., Erban, R., Cao, Y., 2018. Reaction time for trimolecular reactions in compartment-based reaction-diffusion models. *Journal of Chemical Physics*, **148**, 204108.
- [20] Tyson, J. J., 1973. Some further studies of nonlinear oscillations in chemical systems. *The Journal of Chemical Physics*, **58**, 3919.
- [21] Cook, G. B., Gray, P., Knapp, D. G., Scott, S. K., 1989. Bimolecular routes to cubic autocatalysis. *The Journal of Chemical Physics*, **93**: 2749–2755.
- [22] Samardzija, N., Greller, L. D., Wasserman, E., 1989. Nonlinear chemical kinetic schemes derived from mechanical and electrical dynamical systems. *Journal of Chemical Physics*, **90**: 2296–2304.
- [23] Schneider, K. R., and Wilhelm, T., 1998. Model reduction by extended quasi-steady-state approximation. *Weierstraß-Institut für Angewandte Analysis und Stochastik*, Preprint Number 457, Berlin.
- [24] Wilhelm, T., 2000. Chemical systems consisting only of elementary steps - a paradigm for nonlinear behavior. *Journal of Mathematical Chemistry*, **27**: 71–88.
- [25] Kerner, E. N., 1981. Universal formats for nonlinear ordinary differential systems. *Journal of Mathematical Physics*, **22**: 1366–1371.
- [26] Kowalski, K., 1993. Universal formats for nonlinear dynamical systems. *Chem. Phys. Lett.*, **209**: 167–170.
- [27] Weitz, M., Kim, J., Kapsner, K., Winfree, E., Franco, E., Simmel, F. C., 2014. Diversity in the dynamical behaviour of a compartmentalized programmable biochemical oscillator. *Nature Chemistry*, **6**: 295–302.
- [28] Genot, A. J., Baccouche, A., Sieskind, R., Aubert-Kato, N., Bredeche, N., Bartolo, J. F., et al., 2016. High-resolution mapping of bifurcations in nonlinear biochemical circuits. *Nature Chemistry*, 10.1038/nchem.2544.
- [29] Gillespie, D. T., 1992. A rigorous derivation of the chemical master equation. *Physica A: Statistical Mechanics and its Applications*, **188**(1): 404–425.

- [30] Janssen, J., 1989. The elimination of fast variables in complex chemical reactions. II. Mesoscopic level (reducible case). *Journal of Statistical Physics*, **57**: 171–185.
- [31] Thomas, P., Straube, A. V., and Grima, R., 2011. Communication: limitations of the stochastic quasi-steady-state approximation in open biochemical reaction networks. *The Journal of Chemical Physics*, **135**(18): 181103.
- [32] Kim, J., Josic, K., and Bennett, M., 2014. The validity of quasi-steady-state approximations in discrete stochastic simulations. *Biophysical Journal*, **107**: 783–793.
- [33] Agarwal, A., Adams, R., Castellani, G. C., and Shouval, H. Z., 2012. On the precision of quasi steady state assumptions in stochastic dynamics. *The Journal of Chemical Physics*, **137**: 044105.
- [34] Mastny, E. A., Hasteltine, E. L., and Rawlings, J. B., 2007. Two classes of quasi-steady-state model reductions for stochastic kinetics. *The Journal of Chemical Physics*, **127**(9): 094106.
- [35] Rao, C. V., and Arkin, A. P., 2002. Stochastic chemical kinetics and the quasi-steady-state assumption: application to the Gillespie algorithm. *The Journal of Chemical Physics*, **118**: 4999–5010.
- [36] Anderson, D. F., Kurtz, T. G. *Stochastic analysis of biochemical systems*. Springer, 2015.
- [37] Van Kampen, N. G. *Stochastic processes in physics and chemistry*. Elsevier, 2007.
- [38] Gardiner, C. *Handbook of stochastic methods for physics, chemistry, and the natural sciences*. Springer series in synergetics, Springer, New York, 2004.
- [39] Pavliotis, G. A., Stuart, A. M. *Multiscale methods: Averaging and homogenization*. Springer, New York, 2008.